Supporting information for:

Tailorable Plasmonic Circular Dichroism Properties of Helical Nanoparticle Superstructures

Chengyi Song[†], Martin G. Blaber[⊥], Gongpu Zhao[§], Peijun Zhang[§], H. Christopher Fry[#], George C. Schatz[⊥], and Nathaniel L. Rosi*[†]

[†]Department of Chemistry, University of Pittsburgh, 219 Parkman Ave., Pittsburgh, PA 15260, USA, [⊥]Department of Chemistry, Northwestern University, 2145 Sheridan Rd., Evanston, IL 60208, USA, [§]Department of Structural Biology, University of Pittsburgh, School of Medicine, 3501 5th Ave., Pittsburgh, PA 15260, [#]Center for Nanoscale Materials, Argonne National Laboratory, 9700 South Cass Ave., Argonne, IL 60439.

**Corresponding author: nrosi@pitt.edu*

Table of Contents

1. Materials and General Methods

All solvents and chemicals were obtained from commercial sources and used without further purification. 0.1M HEPES Buffer (HEPES = 4-(2-hydroxyethyl)-1-piperazineethanesulfonic acid) was made by directly diluting 1.0M HEPES buffer (pH = 7.3 ± 0.1; Fisher Scientific) with water (NANOpure, Barnstead DiamondTM System.; 18.2 MΩ). 0.1 M citrate buffer was made using citric acid powder (pH = 7.3 ± 0.1, pH was adjusted with NaOH) and NANOpure water. Peptides with sequences of all L amino acids AYSSGAPPMPPF (L-PEP_{Au}) and all D amino acids AYSSGAPPMPPF (D-PEP_{Au}) were synthesized and purified by New England Peptide and Argonne National Laboratory, respectively, with final purity of 99%. Reverse-phase high-pressure liquid chromatography (HPLC) was performed at ambient temperature with an Agilent 1200 liquid chromatographic system equipped with diode array and multiple wavelength detectors using a Grace Vydac protein C4 column (214TP1010, 1.0 cm × 25 cm). Matrix-assisted laser desorption ionization time-of-flight (MALDI-TOF) mass spectra were obtained on an Applied Biosystem Voyager System 6174 MALDI-TOF mass spectrometer using α-cyano-4-hydroxy cinnamic acid (CHCA) as the matrix. Transmission electron microscopy (TEM) samples were prepared by depositing one drop of solution (5 μl) onto a 3-mm-diameter copper grid coated with Formvar/Carbon film. After deposition, the excess solution was wicked from grid with a piece of filter paper. Then, the grid was washed with NANOpure water. TEM analysis was conducted on a JEOL 200CX instrument operated at 200 kV and images were collected using a Gatan charge-coupled device (CCD) image system. STEM was performed on the JEM-2100F HR-TEM operated with a Schottky field-emission electron gun (FEG) at 200 kV and images were collected using a Gatan CCD image system. The projection images from electron tomography studies were recorded with a Gatan 4K × 4K CCD camera mounted on a Tecnai F20 electron microscope (FEI Corporation, Hillsboro, Oreg.) equipped with a field emission gun (FEG) operating at 200 kV. For electron tomography, a series of images were recorded at room temperature at a nominal magnification of 80,000 x by tilting the specimen from −56° to 70° in increments of 1°. Images were recorded at an underfocus value of 1.5 μm along the tilt axis. A back-projection algorithm, as implemented in the IMOD reconstruction package[1], was used to convert the information present in the series of tilted projection images into three-dimensional density maps. The surface rendering was generated using the UCSF Chimera software[2]. Circular dichroism measurements were conducted on a Olis DSM 17 CD

spectrometer. The scan rate was 8 nm/min. All CD experiments were carried out in a 0.08 M HEPES and 0.02 M citrate buffer (pH=7.3±0.1) with a quartz cuvette (0.1 cm path length) at 25 °C.

2. Preparation of N-hydroxyl-succinimide ester and peptide conjugates

Preparation of N-hydroxyl-succinimide ester. Dodecanoic acid (1.200 g, 6.0 mmol) and N-hydroxysuccinimide (0.730 g, 6.3 mmol) were dissolved in 30 mL dry $CH_3COOC_2H_5$. After addition of dicyclohexyl carbodiimide (DCC) (1.47 g, 6.6 mmol) at 0ºC, the solution was stirred overnight at room temperature. The reaction mixture was processed by removing the precipitate via filtration. The solvent was removed under reduced pressure and the residue was recrystallized from isopropanol (iPrOH) to yield the N-hydroxyl-succinimide ester (0.495g, 1.7 mmol, 28%).

Preparation of peptide conjugates. L-AYSSGAPPMPPF (1.26 mg, 1.03×10^{-6} mol) was dissolved in 60 μL DMF. After addition of dodecanoic N-hydroxyl-succinimide ester (0.6 mg, 4.91×10^{-7} mol) in 60μL DMF and 1 μL Et_3N under stirring, the solution was stirred at room temperature for 12 hours. Pure C_{12}-L-PEP_{Au} was obtained by conducting reversed-phase HPLC eluting with a linear gradient of 0.05% formic acid in CH_3CN and 0.1% formic acid in water (5/95 to 95/5 over 30 minutes). The molecular weight for C_{12}-L-PEP_{Au} was confirmed by MALDI-TOF mass spectrometry. Concentration of the peptide was determined spectrophotometrically in water/acetonitrile (1:1) using the molar extinction coefficient of tyrosine (1280 $M^{-1}cm^{-1}$) at 280 nm.

NOTE: C_{12}-D-PEP_{Au} was prepared, purified, and characterized in a similar fashion.

3. Preparation of left- and right-handed gold nanoparticle double helices

A gold ion precursor solution was prepared: 0.1M chloroauric acid ($HAuCl_4$) in 1.0 M triethylammonium acetate (TEAA; pH = 7.0) buffer was incubated for 10 minutes at room temperature. Thereafter, this mixture was centrifuged (10 min., 5K rpm). Lyophilized C_{12}-L-PEP_{Au} (~ 3.75×10^{-8} mol) was completely dissolved in 250 μl 0.08 M HEPES and 0.02 M citrate buffer (pH=7.3±0.1) in a plastic vial. This peptide solution was allowed to incubate for 30 minutes. Thereafter, 2 μl of the supernatant of the centrifuged gold ion precursor solution was

added to the peptide conjugate solution. The mixture was vortexed for a few seconds and then left undisturbed at room temperature for 1 day. Gold nanoparticle double helices were clearly observed as product after ~1 hour.

NOTE: When C_{12}-D-PEP_{Au} was used to prepare right-handed helices similar reaction conditions were employed.

4. Preparation of left-handed double helices comprising small gold nanoparticles

A gold ion precursor solution was prepared: 0.1M chloroauric acid ($HAuCl_4$) in 1.0 M triethylammonium acetate (TEAA; pH = 7.0) buffer was incubated for 10 minutes at room temperature. Thereafter, this mixture was centrifuged (10 min., 5K rpm). Lyophilized C_{12}-L-PEP_{Au} (~ 3.75×10^{-8} mol) was completely dissolved in 250 µl 0.06 M HEPES and 0.04 M citrate buffer (pH=7.3±0.1) in a plastic vial. This peptide solution was allowed to incubate for 30 minutes. Thereafter, 2 µl of the supernatant of the centrifuged gold ion precursor solution was added to the peptide conjugate solution. The mixture was vortexed for a few seconds and then left undisturbed at room temperature for 1 day.

5. Preparation of left- and right-handed double helices comprising large gold nanoparticles

A gold ion precursor solution was prepared: 0.1M chloroauric acid ($HAuCl_4$) in 1.0 M triethylammonium acetate (TEAA; pH = 7.0) buffer was incubated for 10 minutes at room temperature. Thereafter, this mixture was centrifuged (10 min., 5K rpm). Lyophilized C_{12}-L-PEP_{Au} (~ 3.75×10^{-8} mol) was completely dissolved in 250 µl 0.08 M HEPES and 0.02 M citrate buffer (pH=7.3±0.1) in a plastic vial. This peptide solution was allowed to incubate for 30 minutes. Thereafter, 2 µl of the supernatant of the centrifuged gold ion precursor solution was added to the peptide conjugate solution. The mixture was vortexed for a few seconds and then left undisturbed at room temperature for 1 day. At this point, 4 µl of 0.1M chloroauric acid ($HAuCl_4$) aqueous solution was added to the above solution and then vortexed for 5 seconds. After incubation of the above mixture solution for 1 minute, 250 µl 0.1 M Hydroquinone, 0.08 M

HEPES and 0.02 M citrate buffer was added. The mixture solution was vortexed for 3 minutes and the color became dark purple. Double helices with large gold nanoparticles were clearly observed as product after ~1 hour.

NOTE: When C_{12}-D-PEP_{Au} was used, similar reaction conditions were employed.

6. Preparation of silver coated left and right-handed gold nanoparticles double helices

A gold ion precursor solution was prepared: 0.1M chloroauric acid ($HAuCl_4$) in 1.0 M triethylammonium acetate (TEAA; pH = 7.0) buffer was incubated for 10 minutes at room temperature. Thereafter, this mixture was centrifuged (10 min., 5K rpm). Lyophilized C_{12}-L-PEP_{Au} (~ 3.75×10^{-8} mol) was completely dissolved in 250 µl 0.08 M HEPES and 0.02 M citrate buffer (pH=7.3±0.1) in a plastic vial. This peptide solution was allowed to incubate for 30 minutes. Thereafter, 2 µl of the supernatant of the centrifuged gold ion precursor solution was added to the peptide conjugate solution. The mixture was vortexed for a few seconds and then left undisturbed at room temperature for 1 day. A commercially available silver enhancement kit (HQ Silver Enhancement, Nanoprobes, USA) was used for the silver enhancement experiments. There are three kinds of solutions (i.e. “Enhancer”, “Activator” and “Initiator”) provided by the company. “Enhancer”, “Activator”, and “Initiator” solutions were mixed in a 1:1:1 volume ratio. Either 9 µl, 27 µl, 54 µl, or 108 µl of the pre-mixed silver enhancer solution was added to the nanoparticle double helix mixture. The resulting mixtures were vortexed for 3 minutes and then left undisturbed for 1 hour. CD spectra were measured without any further treatment.

NOTE: When C_{12}-D-PEP_{Au} was used, similar reaction conditions were employed.

7. Theoretical modeling of gold nanoparticle double helices

Classical electrodynamics simulations were performed using the Discrete Dipole Approximation (DDA).[3,4] The DDA is an approximate method, but is well known to reproduce essential spectral features[5] of plasmonic nanostructures. Within the framework of the DDA, a target structure is represented by a set of *N* polarizable point dipoles which sit on a cubic lattice. The polarizability, α_i, of the ith point is given by a modified version of the Clausius-Mossotti relationship that relates the macroscopic dielectric function of the metals to the microscopic polarizability of the point dipoles. The modified relationship is often referred to as a lattice dispersion relationship (LDR), and here we have used a version called the Gutkowicz-Krusin & Draine Lattice Dispersion Relation (GKD-LDR)[6] as it corrects for an error in previously published LDRs.[7] Returning to the choice of macroscopic dielectric function, the optical constants of Johnson and Christy[8] were used, after the inclusion of modifications to account for a confined electron mean free path.[9] All simulations were performed in a background medium of water (n=1.333).

In the DDA, the polarizability is used to relate the local electric field at each lattice site, $\mathbf{E}_{loc,i,}$ to the instantaneous dipole moment, $\mathbf{P}_i$, of each dipole: [10]

$$\mathbf{P}_i = \alpha_i \mathbf{E}_{loc,i} \tag{1}$$

The local electric field, $\mathbf{E}_{loc,i}$, at each point is the sum of the incident field, $\mathbf{E}_{inc,i}$, and the fields from the remaining *N*-1 dipoles, $\mathbf{E}_{dip,i}$:

$$\mathbf{E}_{dip,i} = \sum_{j \neq i} \frac{e^{i\mathbf{k}\mathbf{r}_{ij}}}{\mathbf{r}_{ij}^3} \left\{ k^2 \mathbf{r}_{ij} \times (\mathbf{r}_{ij} \times \mathbf{P}_j) + \frac{(1 - i\mathbf{k}\mathbf{r}_{ij})}{\mathbf{r}_{ij}^2} [\mathbf{r}_{ij}^2 \mathbf{P}_j - 3\mathbf{r}_{ij}(\mathbf{r}_{ij}.\mathbf{P}_j)] \right\} = \sum_{j \neq i} \mathbf{A}_{ij}.\mathbf{P}_j \tag{2}$$

where the contribution to the field at position i from the radiating dipole at position j is contained in the 3x3 matrix $\mathbf{A}_{ij}$. The final set of linear equations to be solved can then be written in terms of the incident field, $\mathbf{E}_{inc}$, at the position of each dipole $\mathbf{r}_i$:[11]

$$\mathbf{E}_{\mathrm{inc,i}} = \frac{\mathbf{P}_i}{\alpha_i} + \sum_{j \neq i} \mathbf{A}_{ij}.\mathbf{P}_j \qquad (3)$$

The incident field circularly polarized light is given by $\mathbf{E}_{\mathrm{inc,i}} = \mathbf{e}_H \, e^{i\mathbf{k}\mathbf{r}_i}$ where handedness, *H*, takes values L (left) and R (right), which - for a plane wave propagating in the positive x direction - gives polarization vectors:

$$\mathbf{e}_L = \begin{bmatrix} 0 \\ i \\ 1 \end{bmatrix} / \sqrt{2} \text{ and } \mathbf{e}_R = \begin{bmatrix} 0 \\ 1 \\ i \end{bmatrix} / \sqrt{2} \ . \qquad (4)$$

Selection of Orientations

Simulated CD spectra are very sensitive to the method used to perform orientational averaging. We chose to fix the position and orientation of the helix and rotate the wave vector (**k**) of the incident field for convenience. The list of incident wave vectors was generated using an algorithm that produces quasi-equidistant points on a sphere for an arbitrary number of orientations.[12-15] This ensures that all orientations of the helix with respect to the incident wave vector had equivalent weight. In all the simulations here, we found that 34 wave-vectors on a single octant of the sphere were sufficient to ensure convergence of the CD spectrum.

8. Supplementary data (Figures S1-S33)

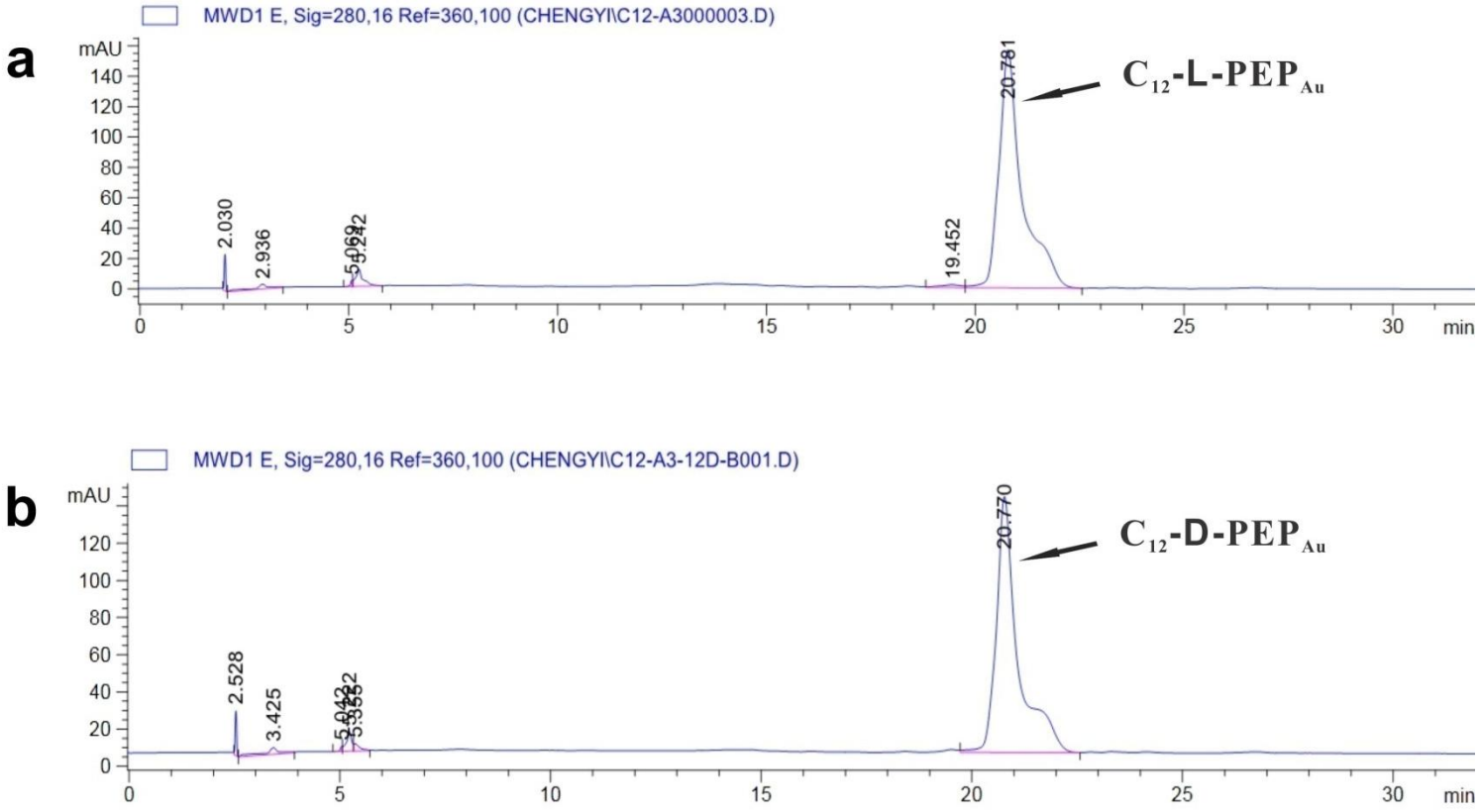

Figure S1.(a) Reverse-phase HPLC chart for the coupling reaction of (L)-AYSSGAPPMPPF with dodecanoic N-hydroxyl-succinimide ester. (b) Reverse-phase HPLC chart for the coupling reaction of (D)-AYSSGAPPMPPF with dodecanoic N-hydroxyl-succinimide ester.

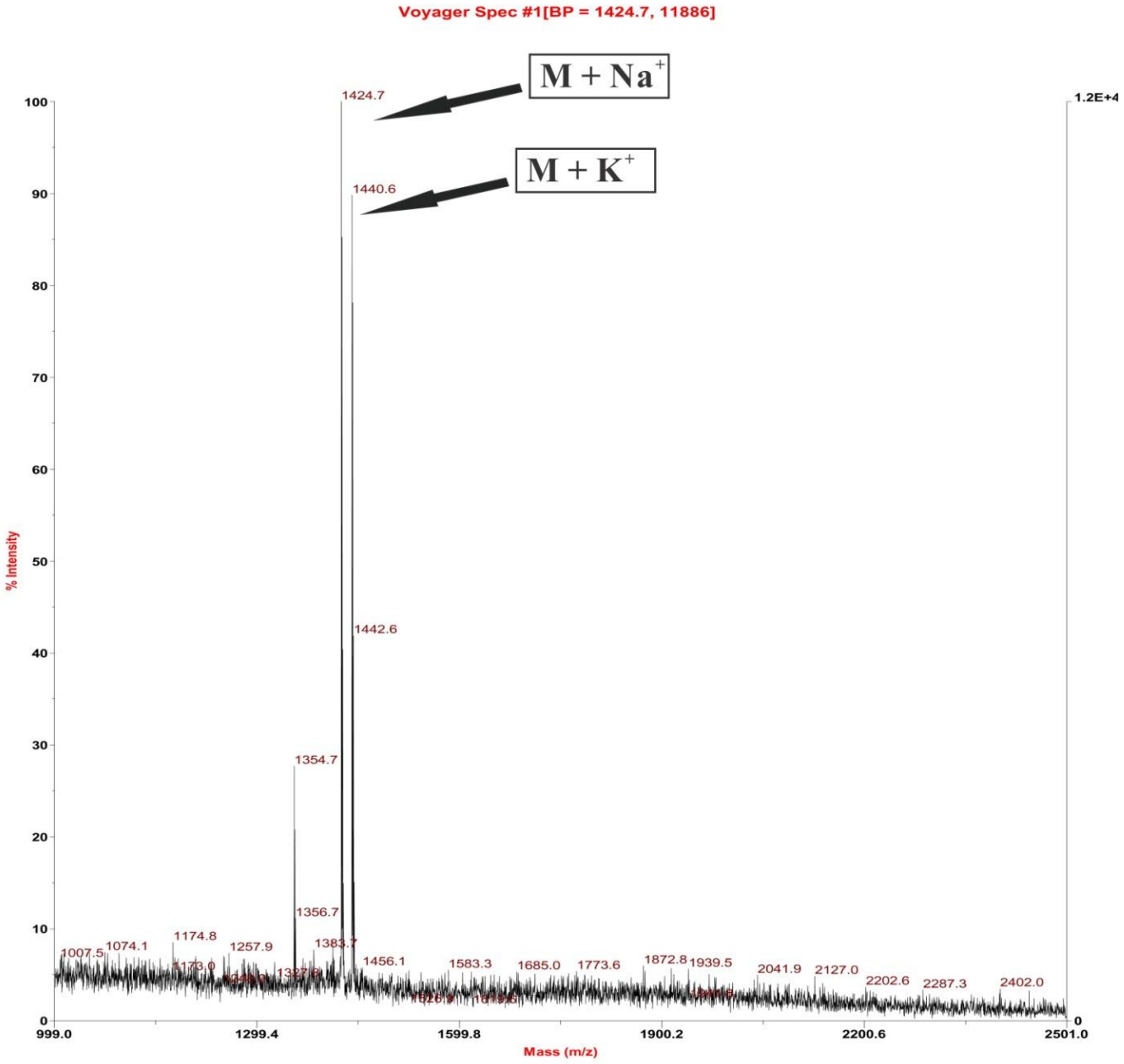

Figure S2. MALDI-TOF mass spectrum of purified C_{12}-L-PEP_{Au}. The molar mass of C_{12}-L-PEP_{Au} is 1403 g/mol. [C_{12}-L-PEP_{Au} + Na^+] = 1424.7 g/ mol and [C_{12}-L-PEP_{Au} + K^+] =1440.6 g/mol.

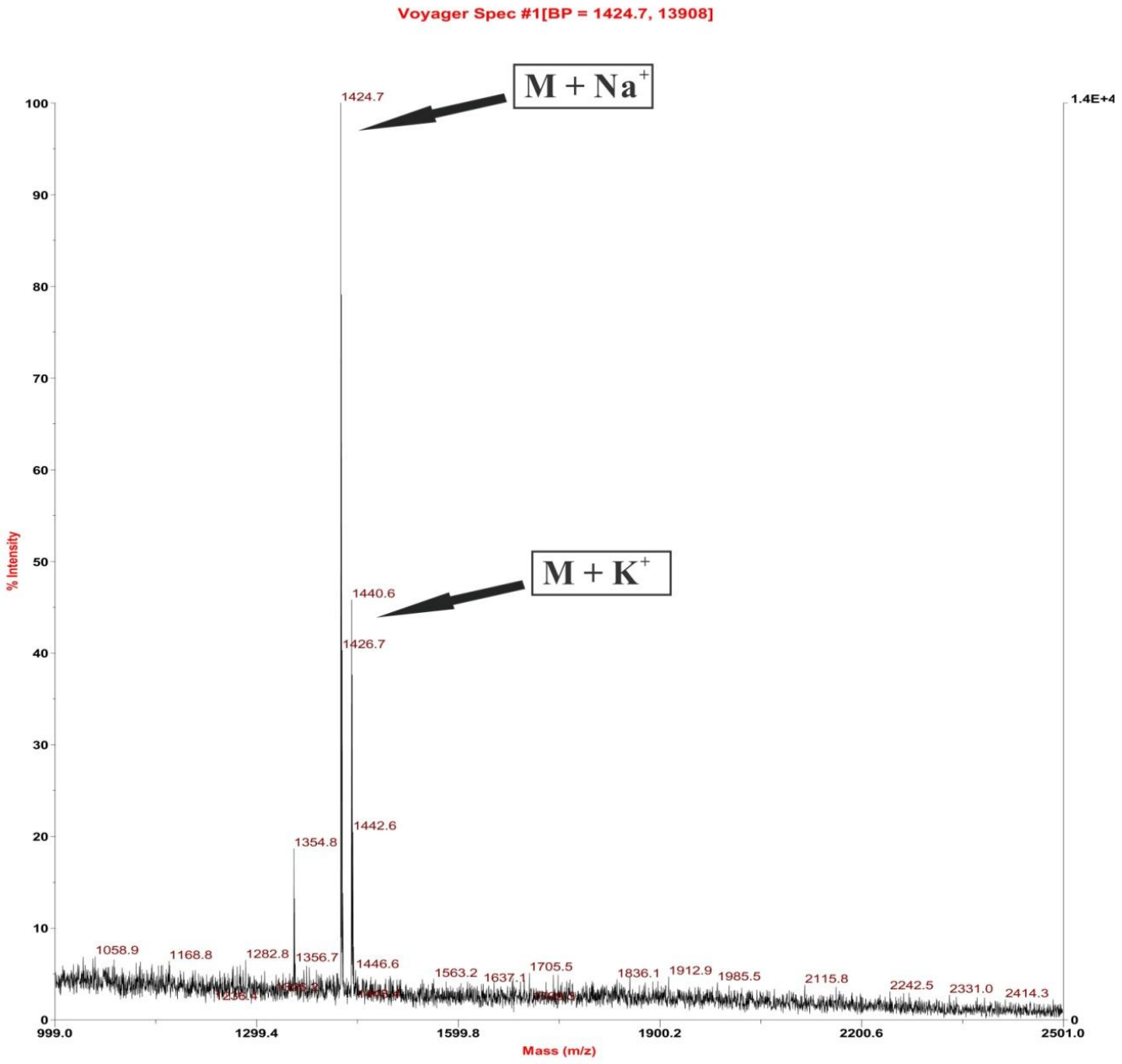

Figure S3. MALDI-TOF mass spectrum of purified C_{12}-D-PEP_{Au}. The molar mass of C_{12}-D-PEP_{Au} is 1403 g/mol. [C_{12}-D-PEP_{Au} + Na^+] = 1424.7 g/ mol and [C_{12}-D-PEP_{Au} + K^+] =1440.6 g/mol.

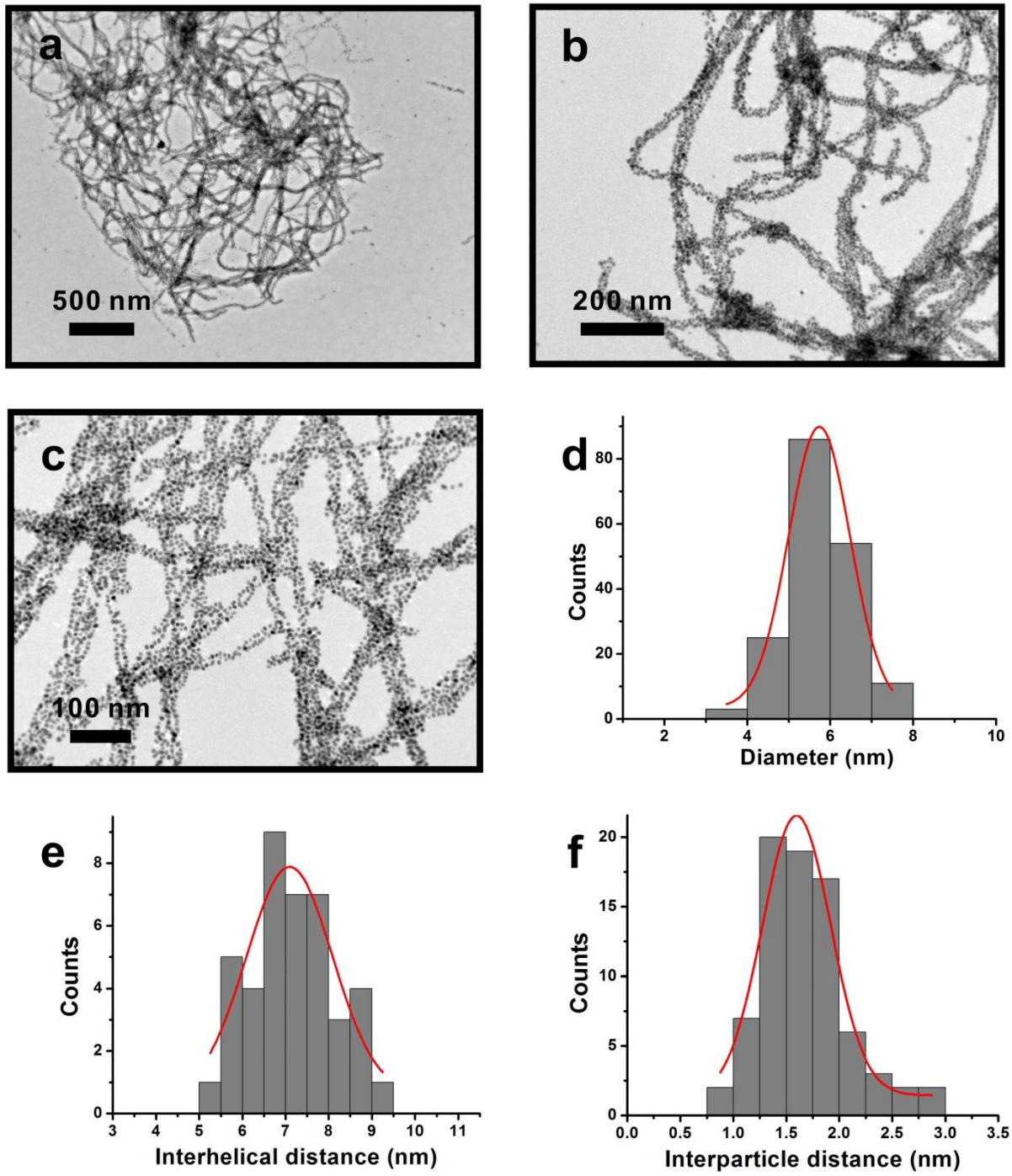

Figure S4. Additional TEM images (a-c) of left-handed nanoparticle double helices after one hour incubation. (d) Distribution of sizes of gold nanoparticles within the double helix (based on 179 counts; diameter = 5.74 ± 0.75 nm). (e) Distribution of the interhelical distance between particles along the width of the left-handed gold nanoparticle double helices (based on 41 counts; distance = 7.09 ± 1.00 nm). (f) Distribution of the edge-to-edge distance between nanoparticles along the longitudinal dimension of the gold nanoparticle double helices (based on 78 counts; distance = 1.60 ± 0.33 nm).

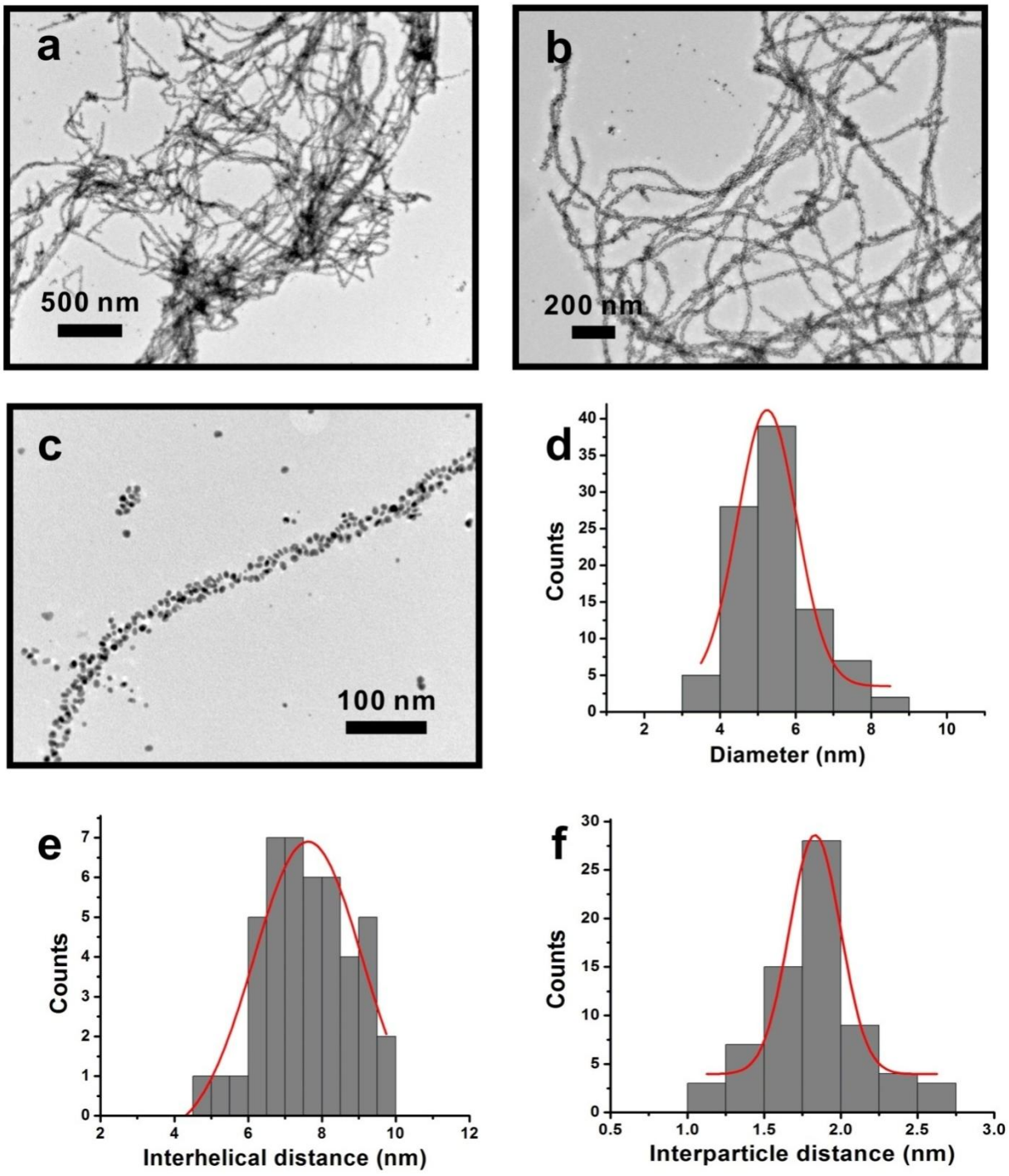

Figure S5. Additional TEM images (a-c) of right-handed nanoparticle double helices after one hour incubation. (d) Distribution of size of gold nanoparticles within the double helix (based on 95 counts; diameter = 5.25 ± 0.79 nm). (e) Distribution of the interhelical distance between particles along the width of the right-handed gold nanoparticle double helices (based on 45 counts; distance = 7.62 ± 1.48 nm). (f) Distribution of the edge-to-edge distance between nanoparticles along the longitudinal dimension of the gold nanoparticle double helices (based on 69 counts; distance = 1.83 ± 0.17 nm).

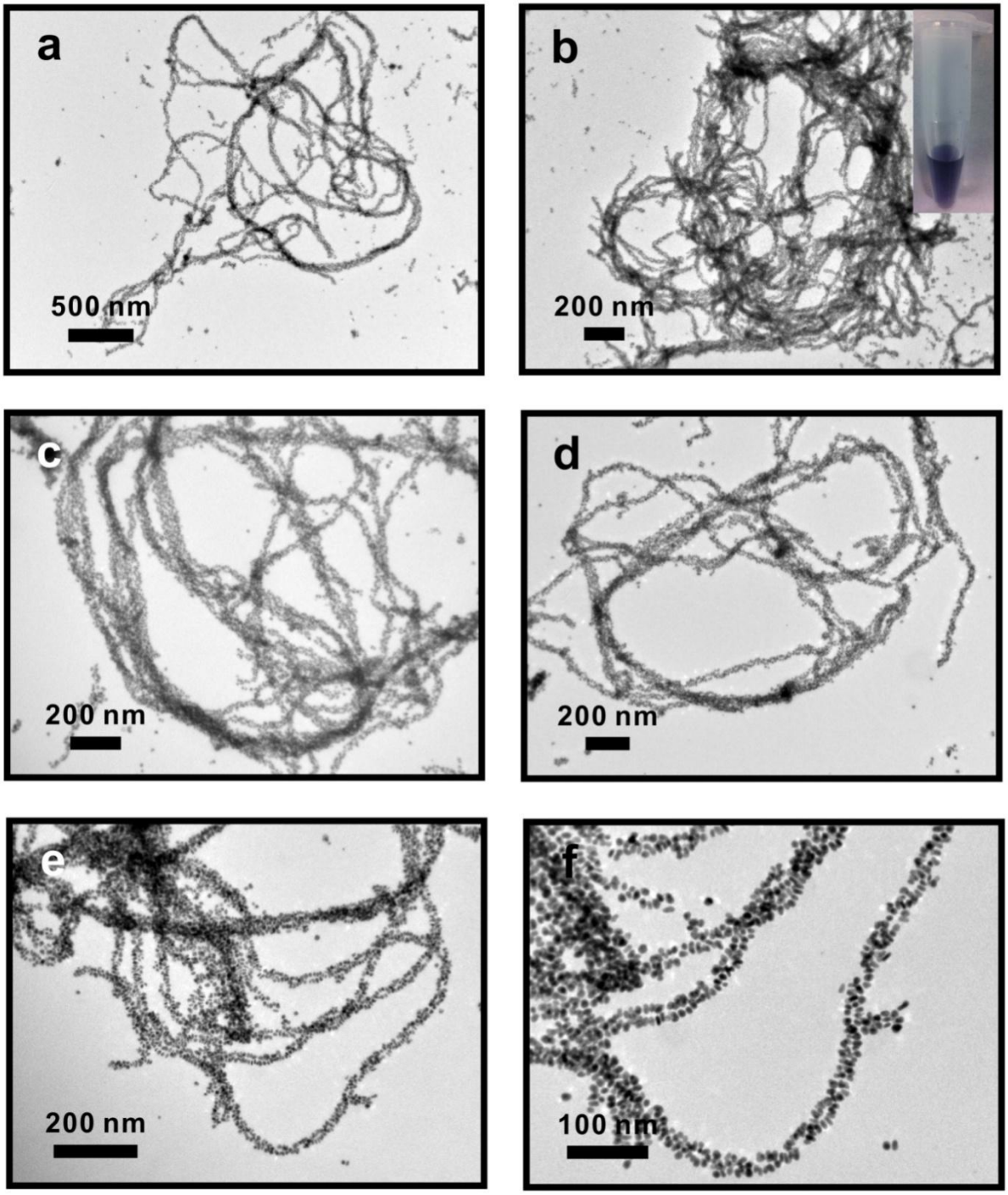

Figure S6. Additional TEM images (a-f) of left-handed gold nanoparticle double helices. The vial in the inset image shows the purple color of the gold nanoparticle double helices solution after one day of incubation.

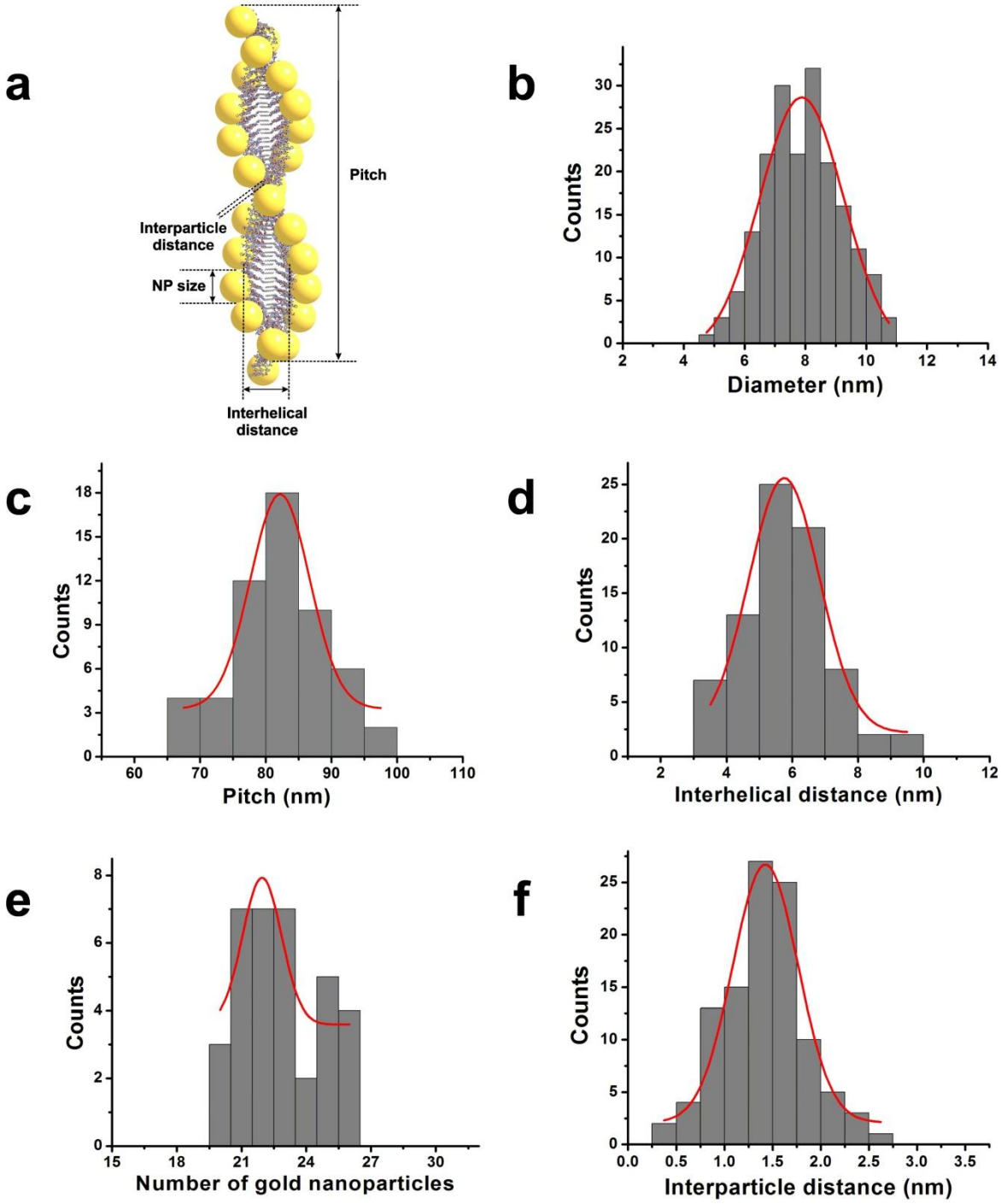

Figure S7. Statistics of left-handed gold nanoparticle double helices after one day incubation based on TEM images. (a) Illustration of left-handed gold nanoparticle double helix with relevant metrics indicated. (b) Distribution of nanoparticle size (based on 188 counts; diameter = 7.88 ± 1.38 nm). (c) Distribution of pitch (based on 56 counts; pitch = 82.17 ± 4.51 nm). (d) Distribution of the interhelical distance (based on 78 counts; distance = 5.75 ± 1.07 nm). (e) Distribution of number of gold nanoparticles per pitch of double helix (based on 35 counts; number = 22 ± 1). (f) Distribution of the edge-to-edge distance between nanoparticles along the longitudinal dimension of the gold nanoparticle double helices (based on 105 counts; distance = 1.43 ± 0.34 nm).

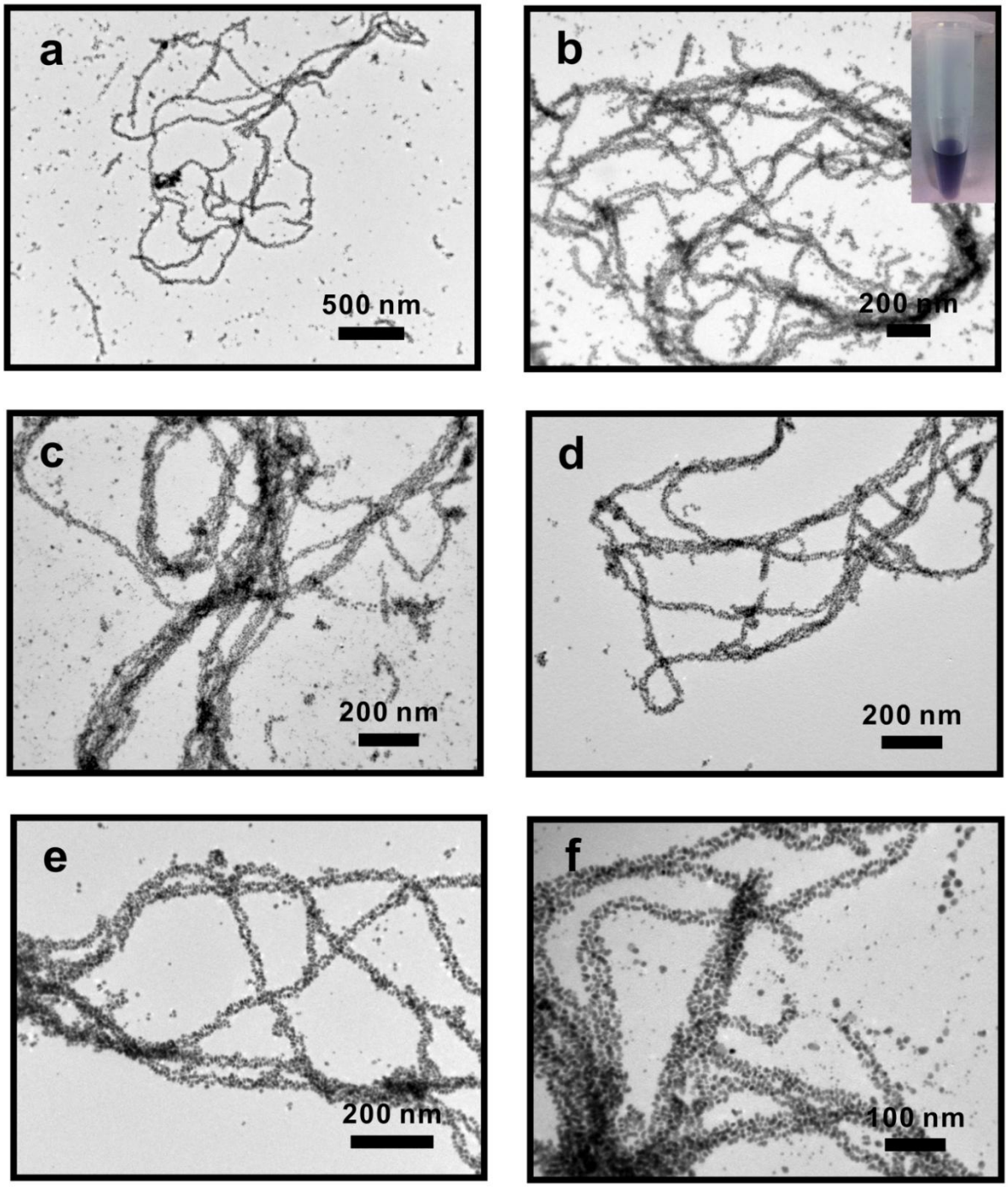

Figure S8. Additional TEM images (a-f) of right-handed gold nanoparticle double helices. The vial in the inset image shows the purple color of gold nanoparticle double helices solution after one day incubation.

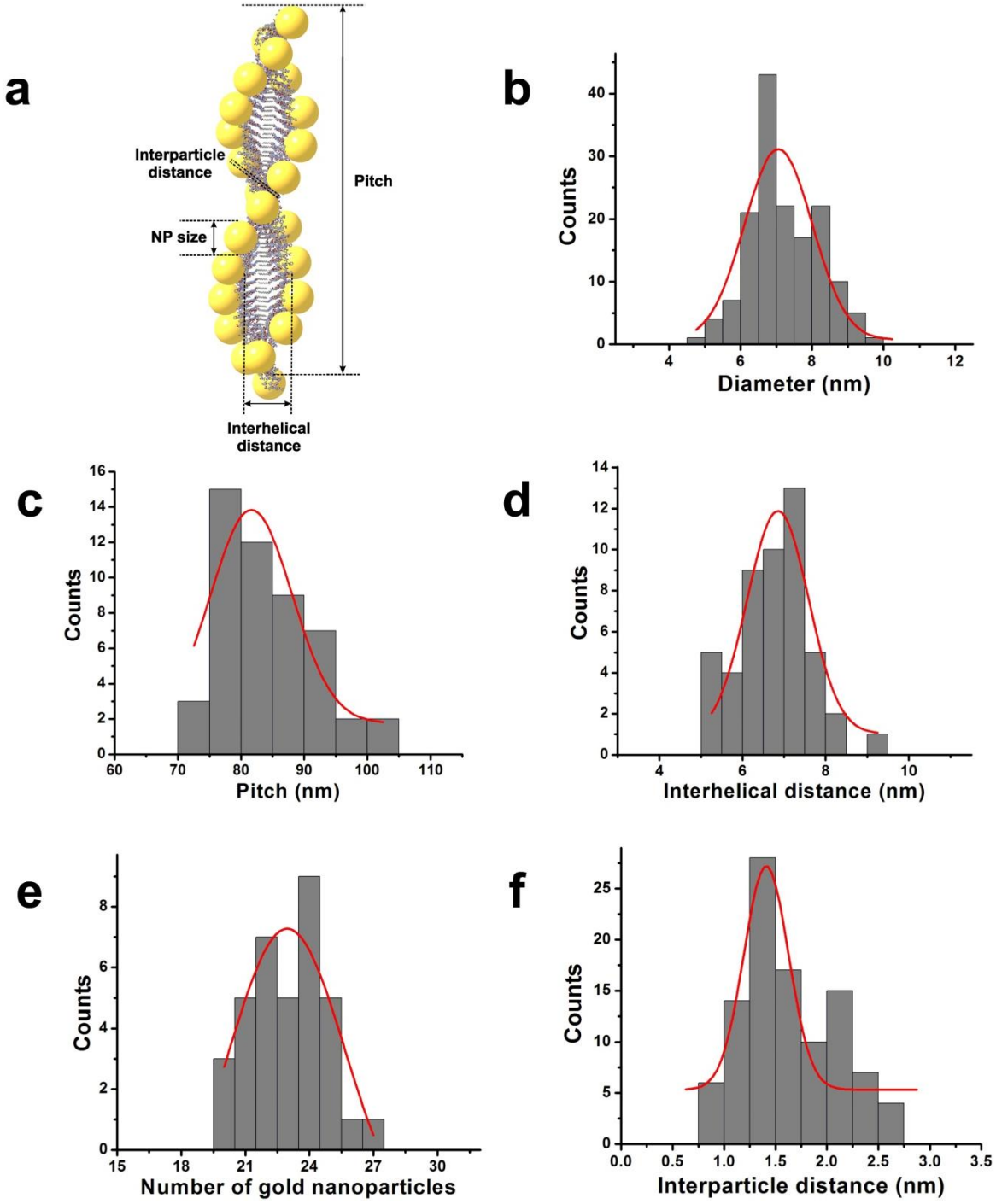

Figure S9. Statistics of right-handed gold nanoparticle double helices after one day incubation based from TEM images. (a) Illustration of right-handed gold nanoparticle double helix with relevant metrics indicated. (b) Distribution of nanoparticle size (based on 153 counts; diameter = 7.06 ± 0.95 nm). (c) Distribution of pitch (based on 50 counts; pitch = 81.64 ± 6.42 nm). (d) Distribution of the interhelical distance (based on 49 counts; distance = 6.85 ± 0.74 nm). (e) Distribution of number of gold nanoparticles per pitch of double helix (based on 36 counts; number = 23 ± 2). (f) Distribution of the edge-to-edge distance between nanoparticles along the longitudinal dimension of the gold nanoparticle double helices (based on 101 counts; distance = 1.41 ± 0.22 nm).

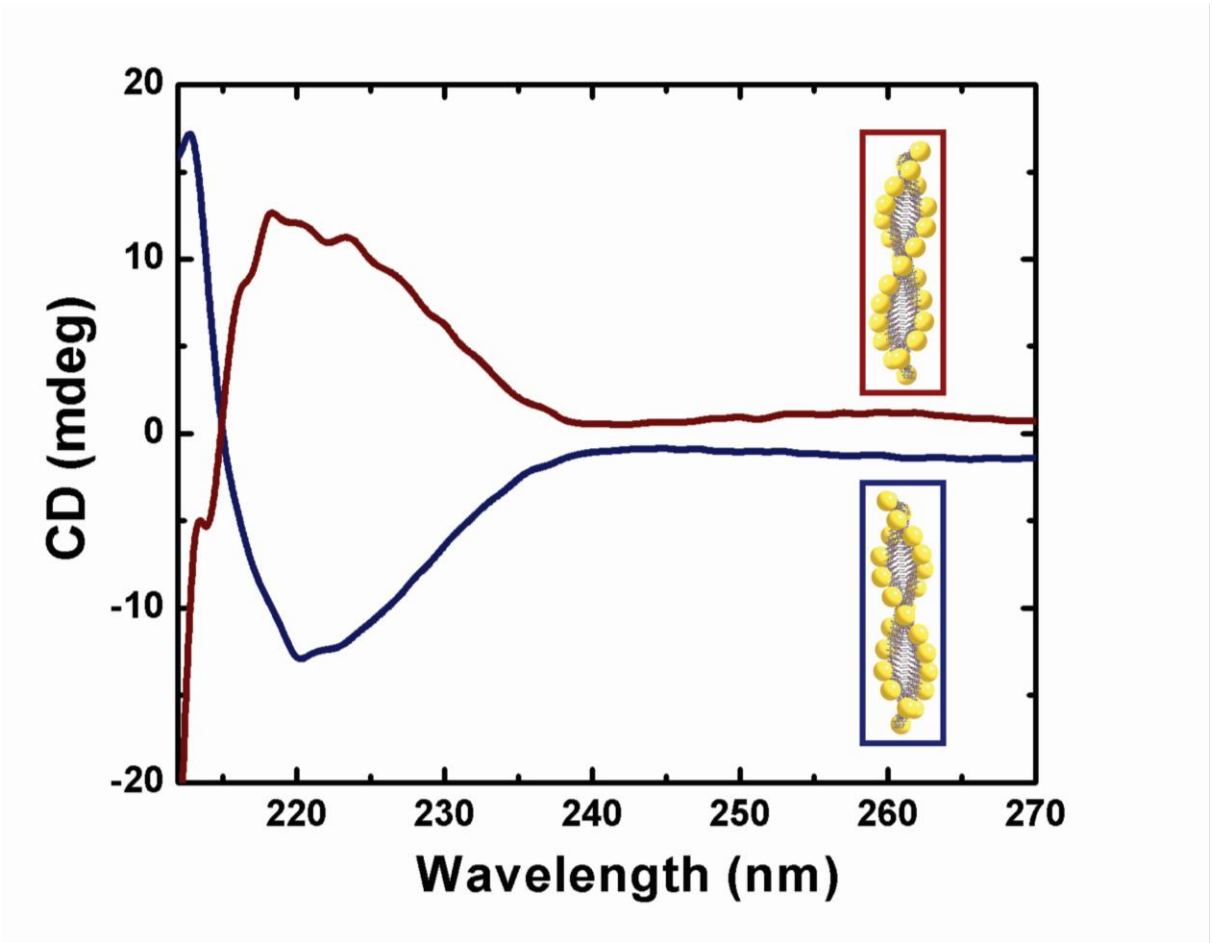

Figure S10. Circular Dichroism (CD) spectra of solutions of left- (blue) and right-handed (red) gold nanoparticle double helices after one day incubation. The path length of the light is 1 mm.

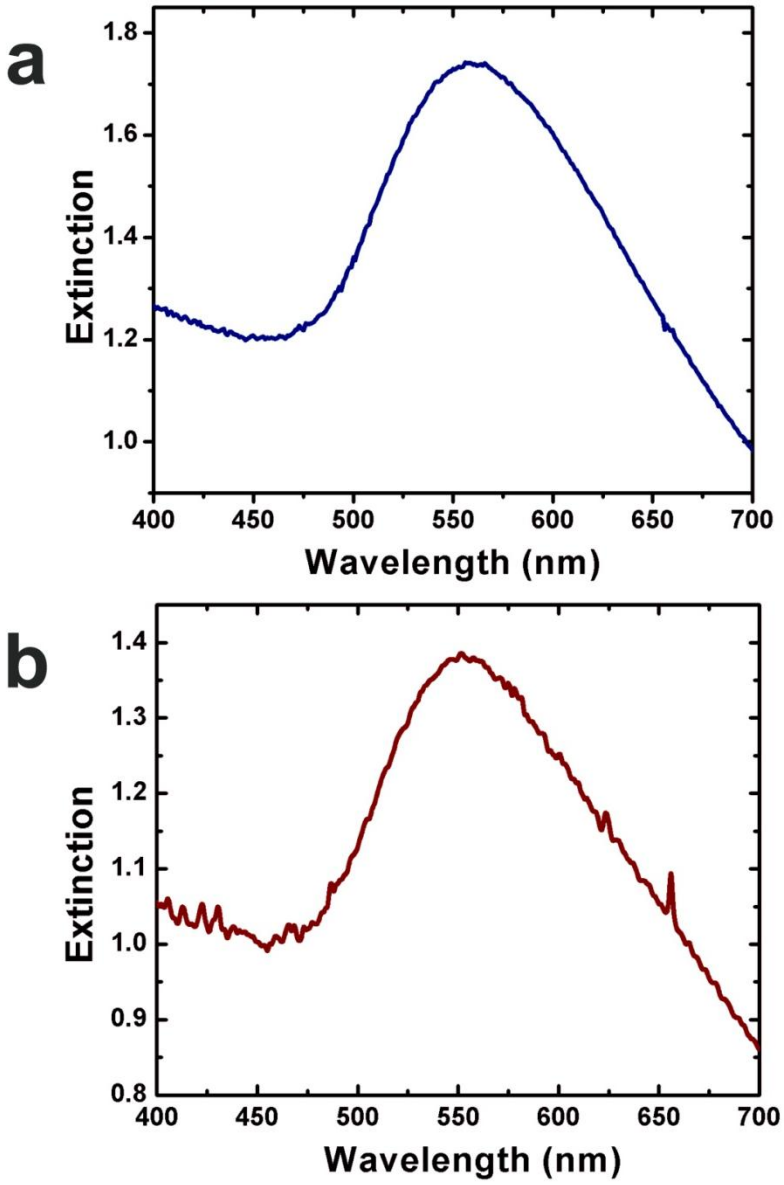

Figure S11. (a) UV-Vis spectrum of left-handed gold nanoparticle double helices in solution after one day incubation. (b) UV-Vis spectrum of right-handed gold nanoparticle double helices in solution after one day incubation. The absorbance maximum is observed at 556 nm (blue) and 552 nm (red), which is consistent with our previous work[16]. The peaks are red-shifted compared to reported monodisperse gold colloidal solutions of nanoparticles similar in size to what we observe within the nanoparticle double helices[17]. This effect results from the coupling of the surface plasmons between assembled gold nanoparticles. The path length of the light is 10 mm.

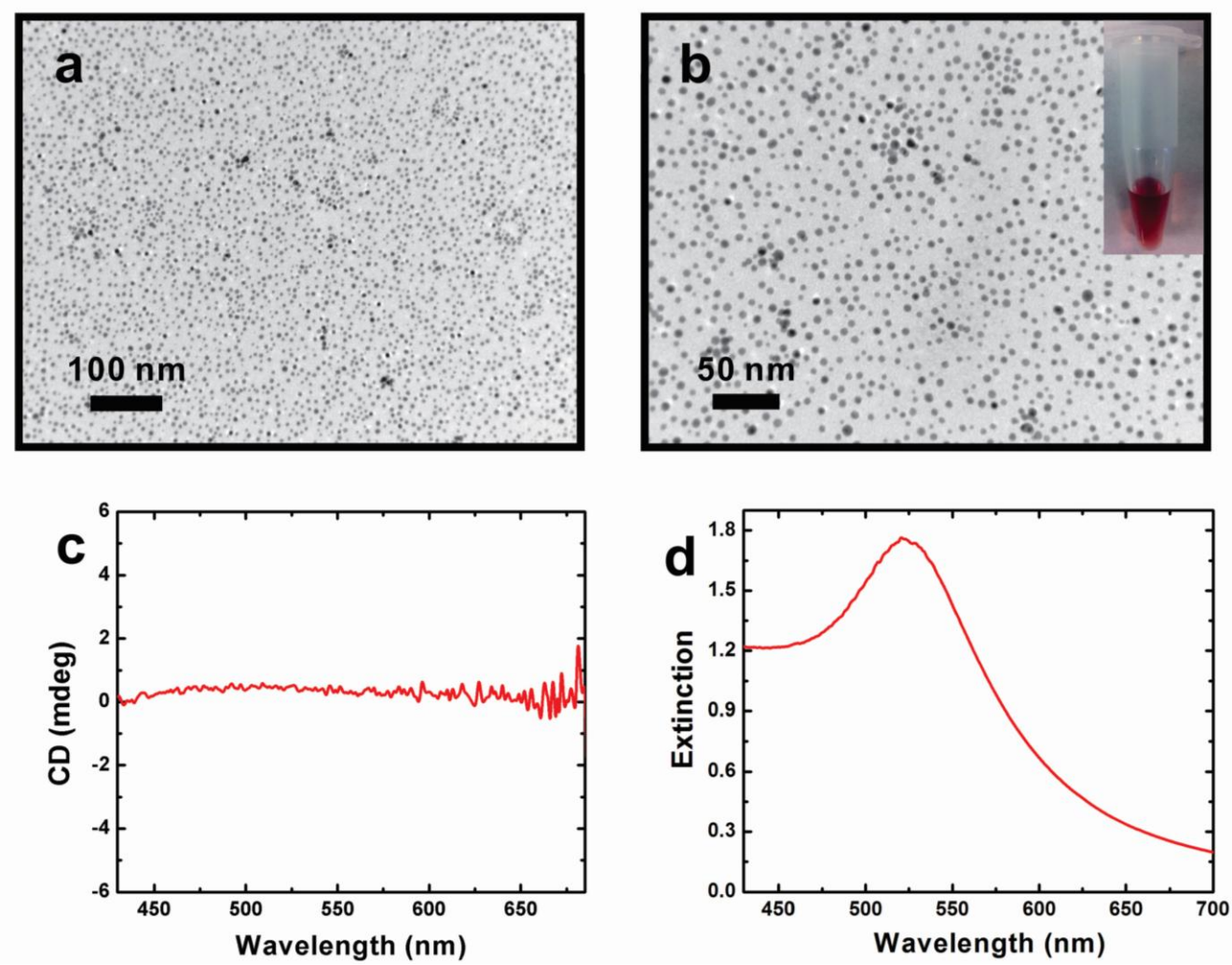

Figure S12. (a),(b) TEM images of free gold nanoparticles formed using PEP_{Au} instead of C_{12}-L-PEP_{Au}. (Inset image shows the typical red colour of the free gold nanoparticle colloidal solution) (c) CD spectrum of the free gold nanoparticle colloidal solution. There is no significant CD feature within the visible light region. The path length of the light is 1 mm. (d) UV-Vis spectrum of the free gold nanoparticle colloidal solution. It shows a typical surface plasmon peak at 520 nm.

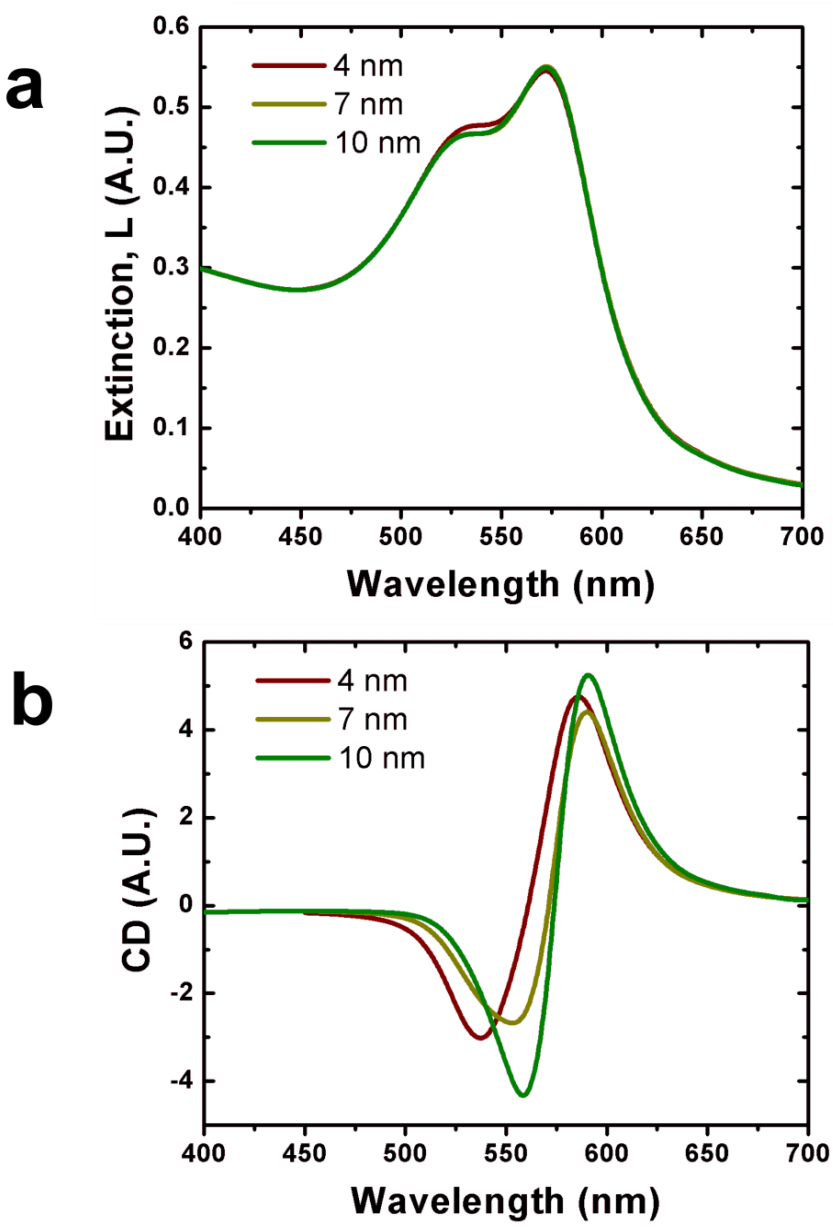

Figure S13. Simulation of the effect of interhelical spacing on CD response. The effect of interhelical spacing on the extinction (a) and CD (b) of a right-handed double helix ensemble comprising 22 spheres. The interhelical spacing was sampled at 4.0 nm, 7.0 nm, the approximate experimental value, and 10.0 nm. The sphere diameter is 8.0 nm and the interparticle spacing is 1.5 nm.

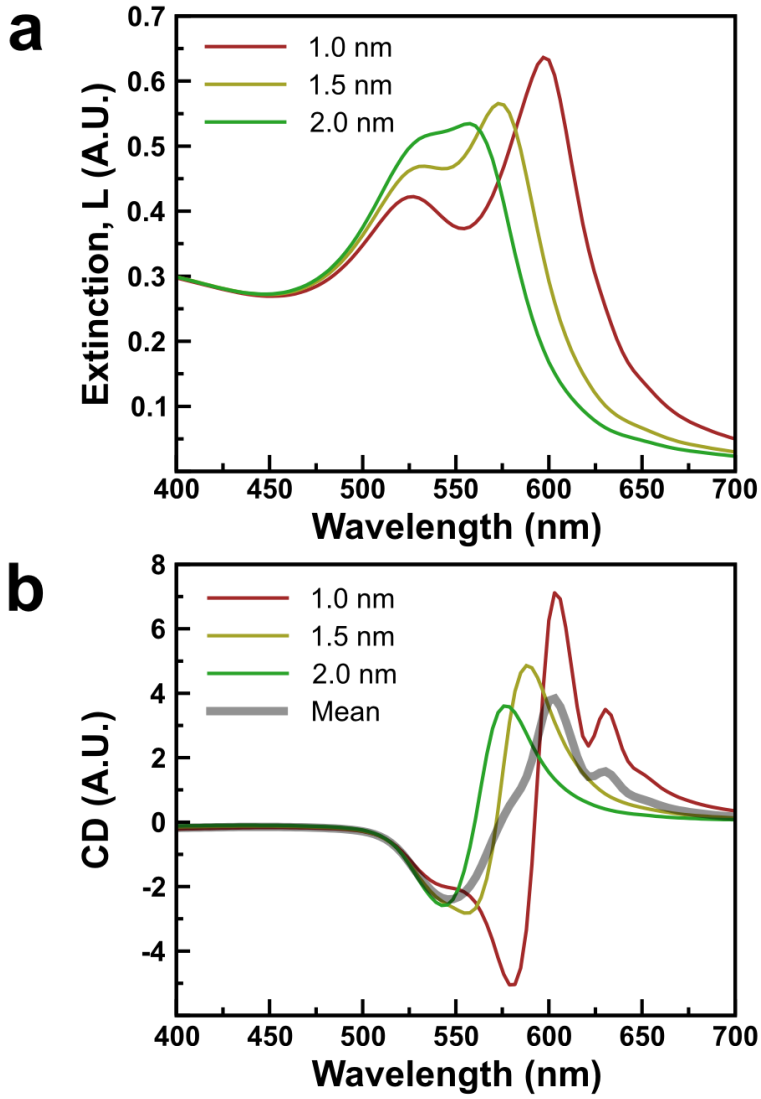

Figure S14. Simulation of the effect of interparticle distance on CD response. The effect of interparticle distance on the extinction (a) and CD (b) of a right-handed double helix ensemble comprising 22 spheres. The double peaks in (a) represent the transverse surface plasmon resonance at around 525 nm (where the incident field polarization is perpendicular to the helical axis), and the longitudinal mode (where the incident field polarization is parallel to the helical axis), which red-shifts as the interparticle spacing decreases. See Equation 2 in the main text. The interparticle distance was sampled at 1.0 nm, 1.5 nm, the approximate experimental value, and 2.0 nm. The interhelical spacing is 7.0 nm and the sphere diameter is 8.0 nm.

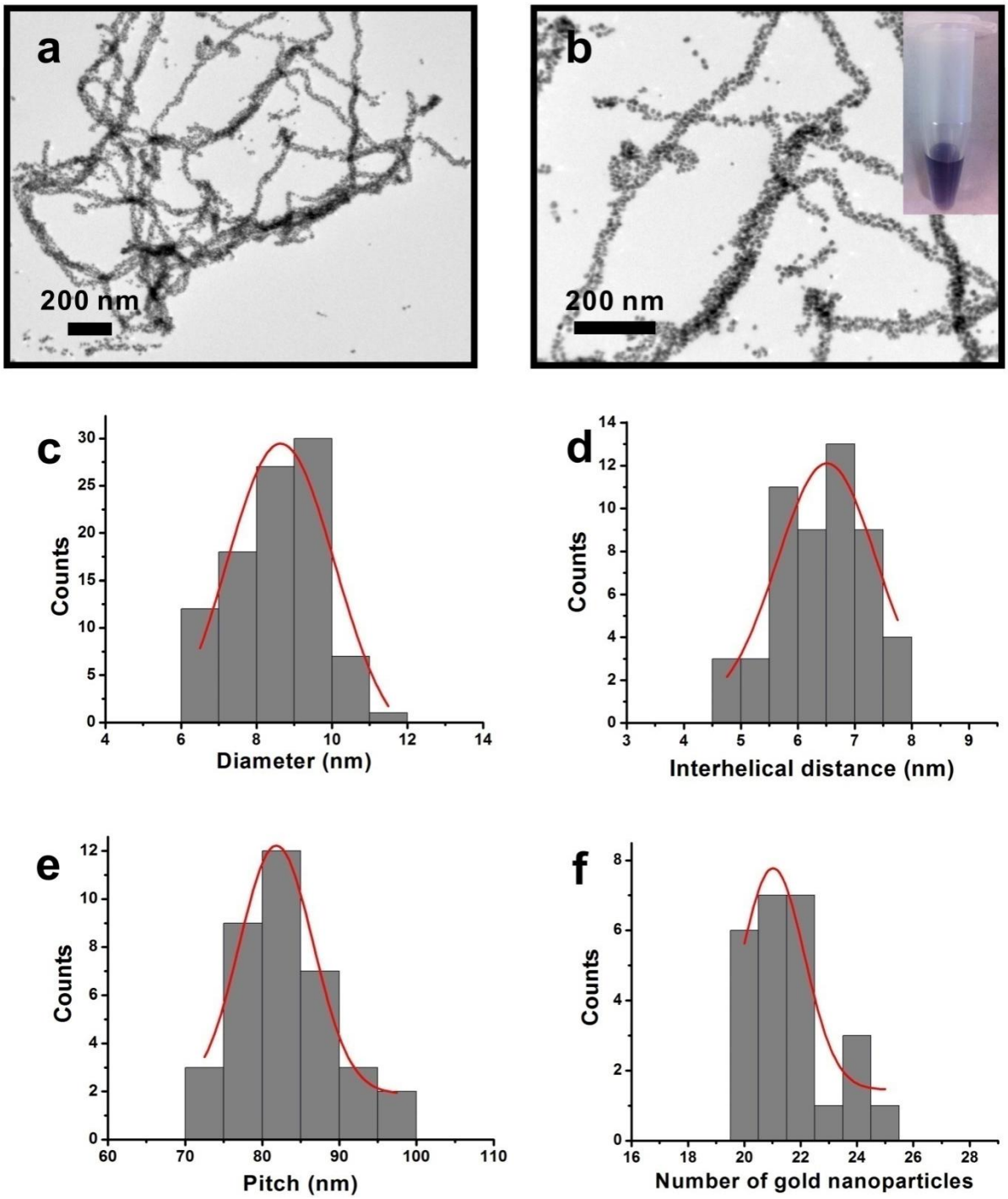

Figure S15. TEM images and statistics of left-handed gold nanoparticle double helices in 0.08 M HEPES and 0.02 M citrate buffer after one day incubation. (a) (b) TEM images of left-handed gold nanoparticle double helices. The inset image of the vial shows the purple color of the gold nanoparticle double helices solution. (c) Distribution of nanoparticle size (based on 95 counts; diameter = 8.64 ± 1.43 nm). (d) Distribution of the interhelical distance (based on 52 counts; distance = 6.51 ± 0.87 nm). (e) Distribution of pitch (based on 36 counts; pitch = 81.83 ± 4.77 nm). (f) Distribution of number of gold nanoparticles per pitch of double helix (based on 25 counts; number = 21 ± 1).

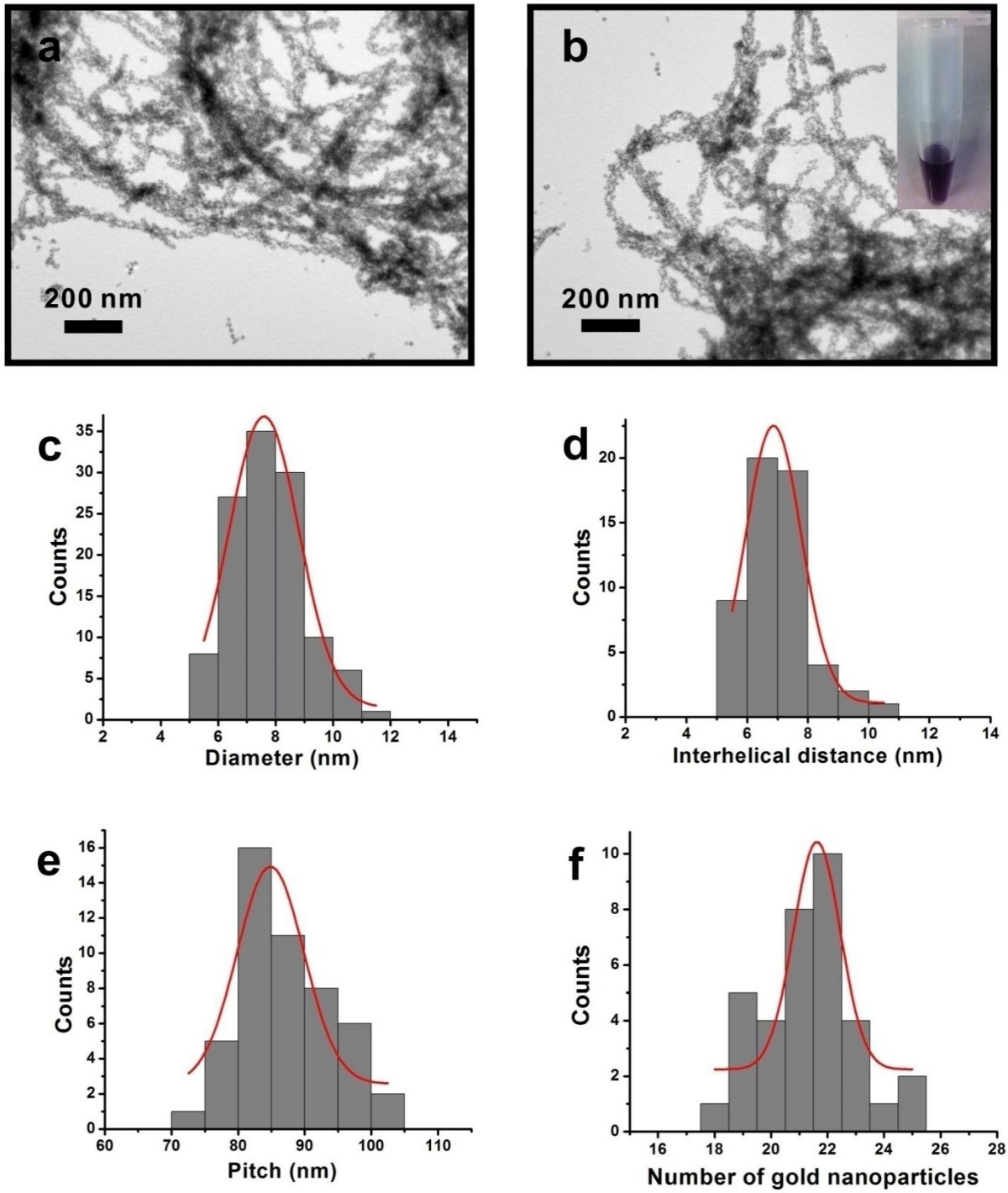

Figure S16. TEM images and statistics of right-handed gold nanoparticle double helices in 0.08 M HEPES and 0.02 M citrate buffer after one day incubation. The inset image of the vial shows the purple color of gold nanoparticle double helices solution. (a) (b) TEM images of right-handed gold nanoparticle double helices. (c) Distribution of nanoparticle size (based on 117 counts; diameter = 7.59 ± 1.22 nm). (d) Distribution of the interhelical distance (based on 55 counts; distance = 6.86 ± 0.92 nm). (e) Distribution of pitch (based on 49 counts; pitch = 84.86 ± 5.00 nm). (f) Distribution of number of gold nanoparticles per pitch of double helix (based on 35 counts; number = 22 ± 1).

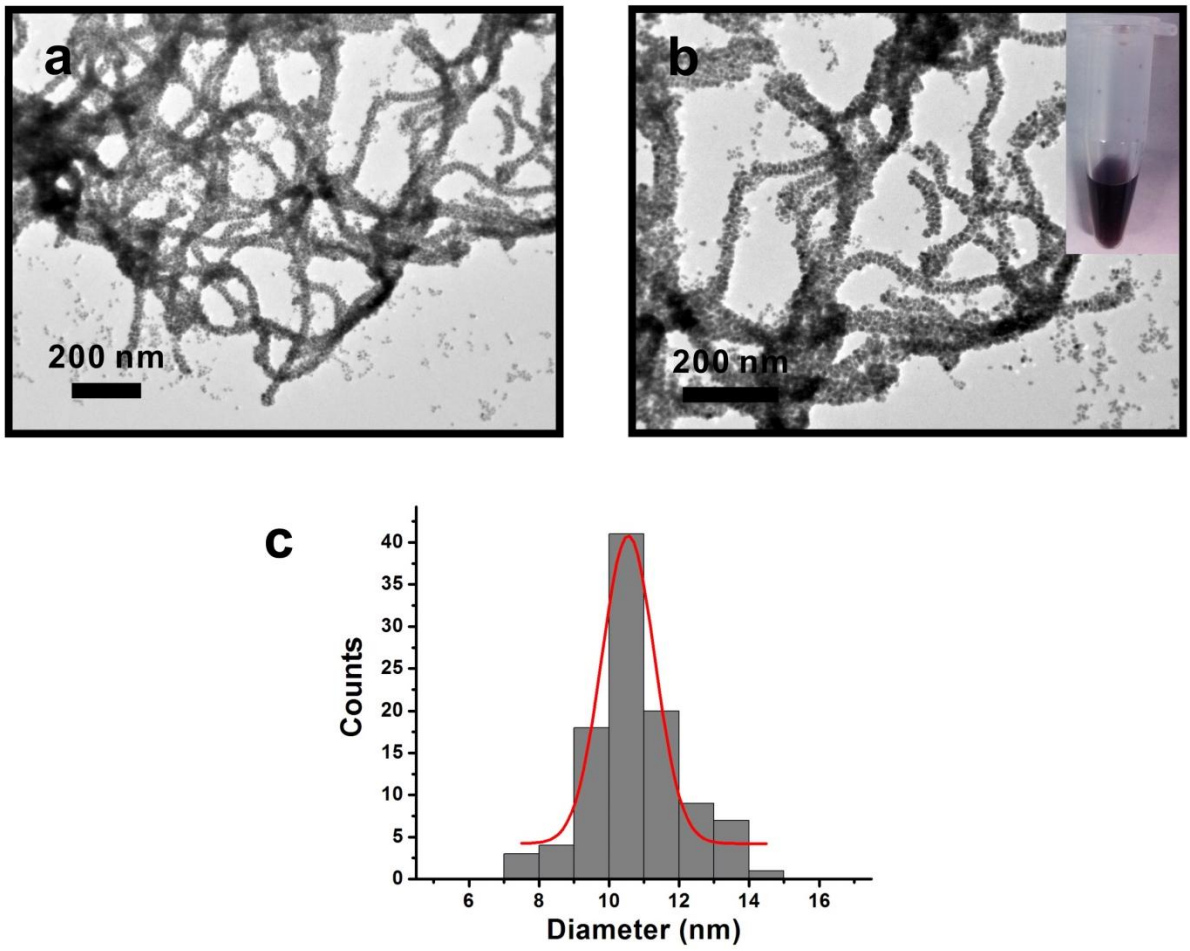

Figure S17. (a-b) TEM images of gold enhanced left-handed nanoparticle double helices. The inset image of the vial shows the dark purple color of gold nanoparticle double helices solution. (c) Distribution of nanoparticle size (based on 100 counts; diameter = 10.55 ± 0.75 nm).

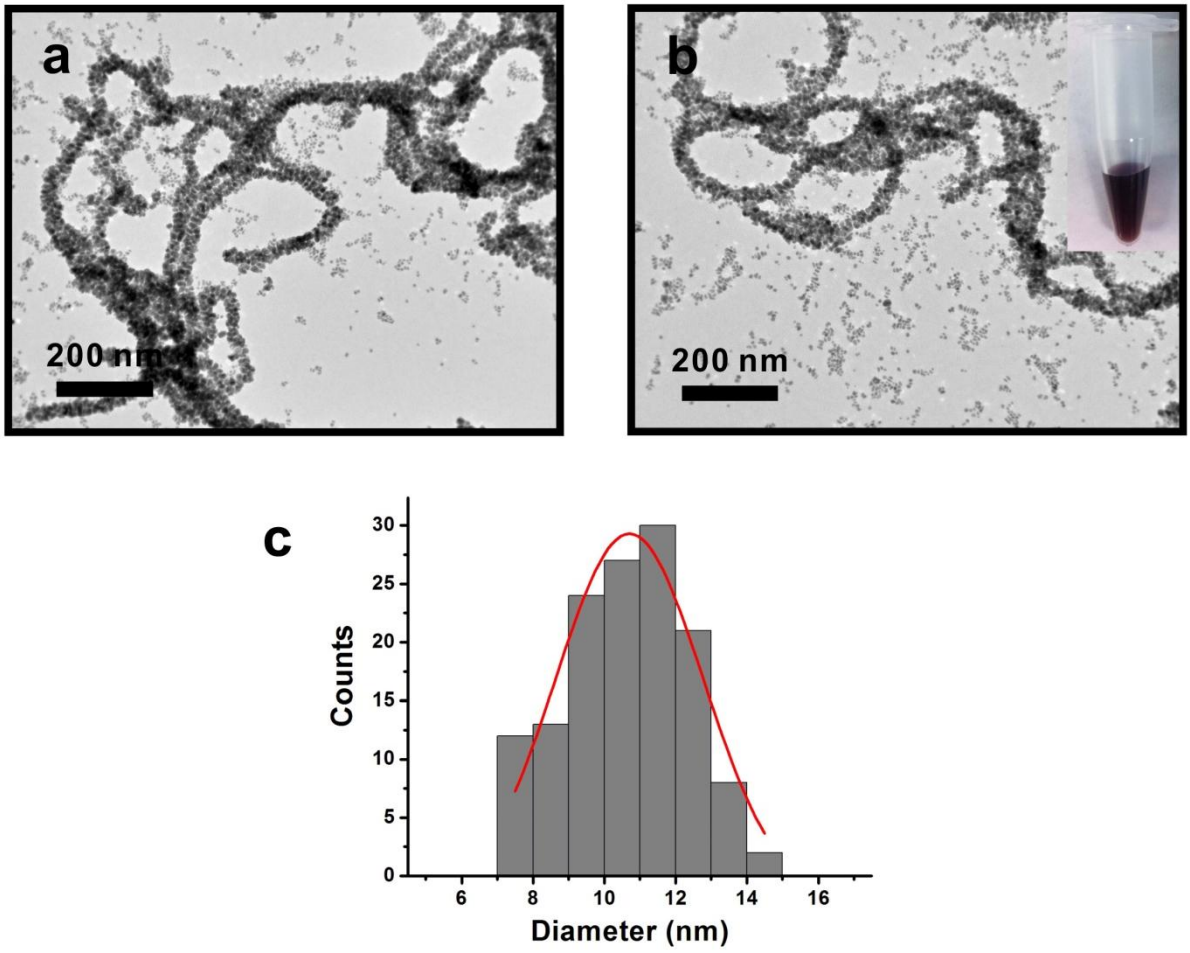

Figure S18. (a-b) TEM images of gold enhanced right-handed nanoparticle double helices. The inset image of the vial shows the dark purple color of gold nanoparticle double helices solution. (c) Distribution of nanoparticle size (based on 137 counts; diameter = 10.70 ± 2.07 nm).

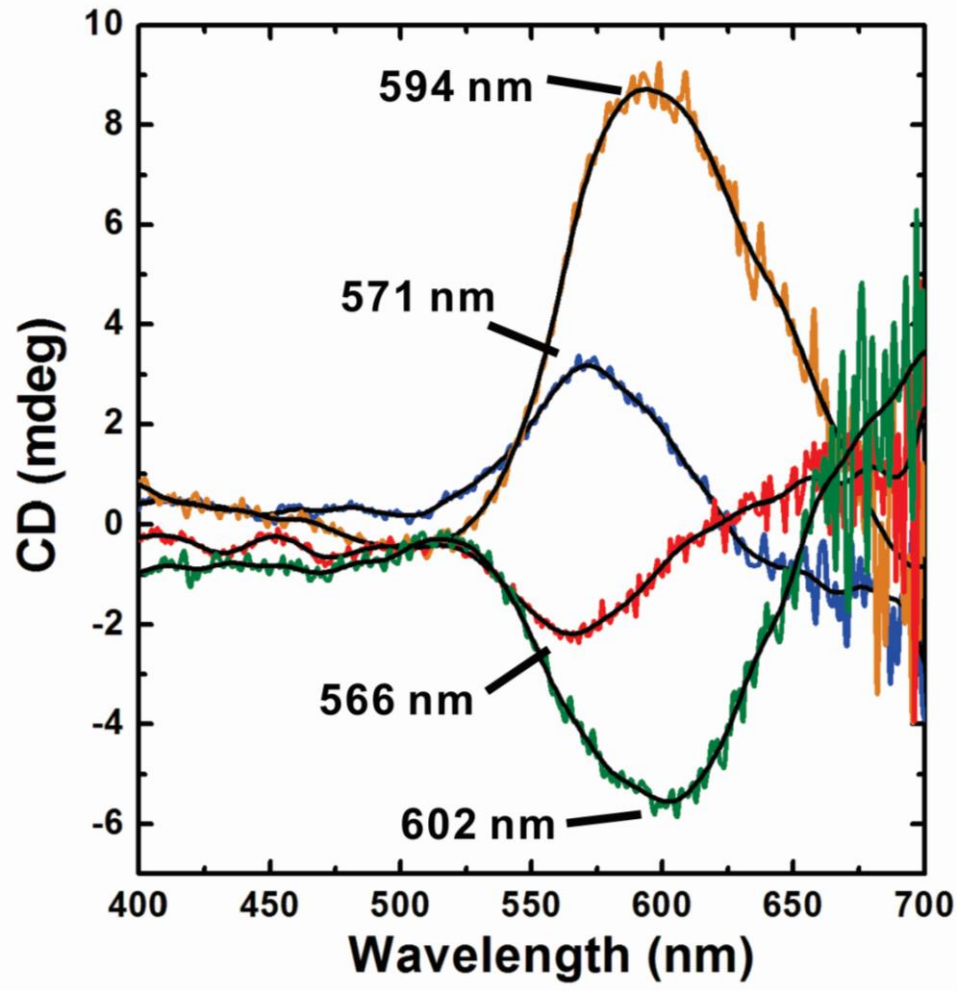

Figure S19. CD spectra of left- and right-handed gold nanoparticle double helices solutions. Blue line: left-handed gold double helices without gold enhancement; Red line: right-handed gold double helices without gold enhancement; Orange line: left-handed gold double helices enhanced by gold aqueous solution; Green line: right-handed gold double helices enhanced by gold aqueous solution. The path length of the light is 1 mm.

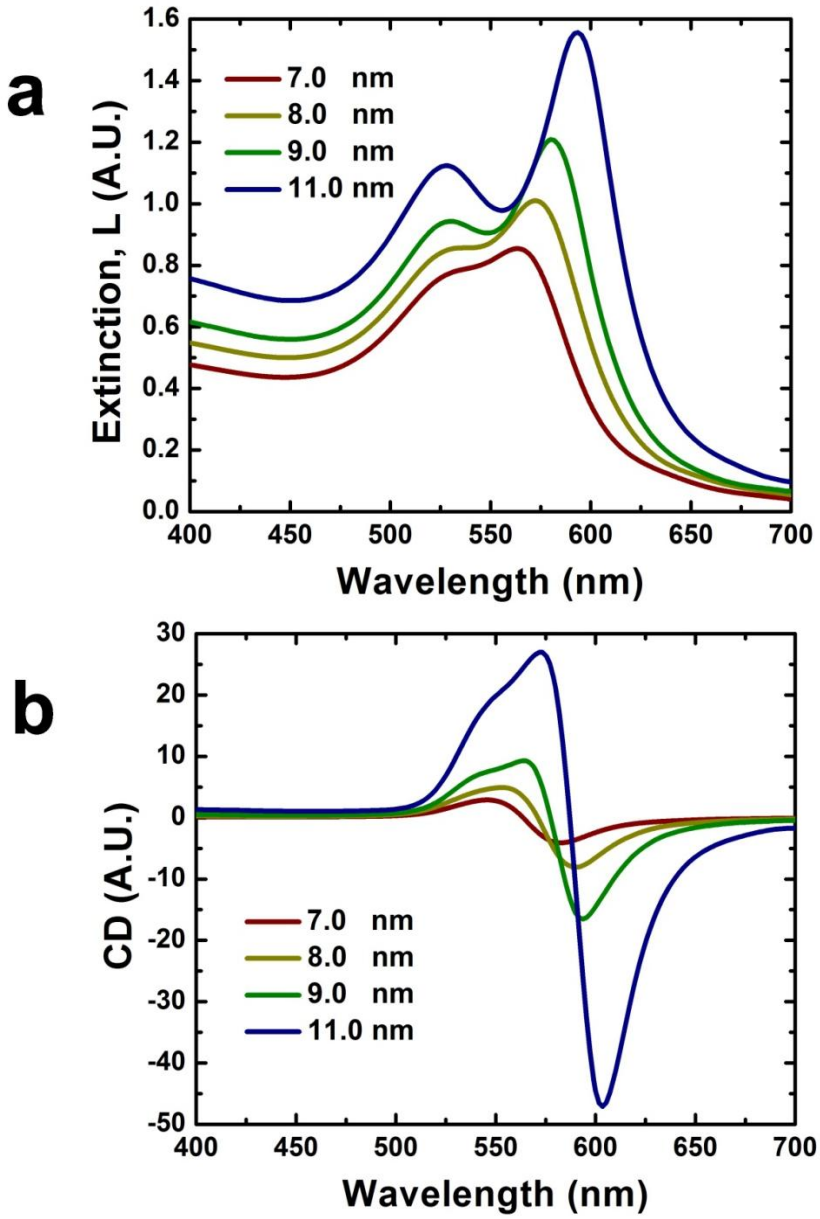

Figure S20. Simulation of the effect of sphere diameter on CD response. The effect of sphere diameter on the extinction (a) and CD (b) of a left-handed double helix ensemble comprising 22 spheres. The double peaks in (a) represent the transverse surface plasmon resonance at around 525 nm (where the incident field polarization is perpendicular to the helical axis), and the longitudinal mode (where the incident field polarization is parallel to the helical axis), which red-shifts as the particle size increases. See Equation 2 in the main text. The sphere diameter was sampled at 7.0 nm, 8.0 nm, the approximate experimental value, 9.0 nm and 11.0 nm. The interhelical distance is 7.0 nm and the interparticle distance is 1.5 nm.

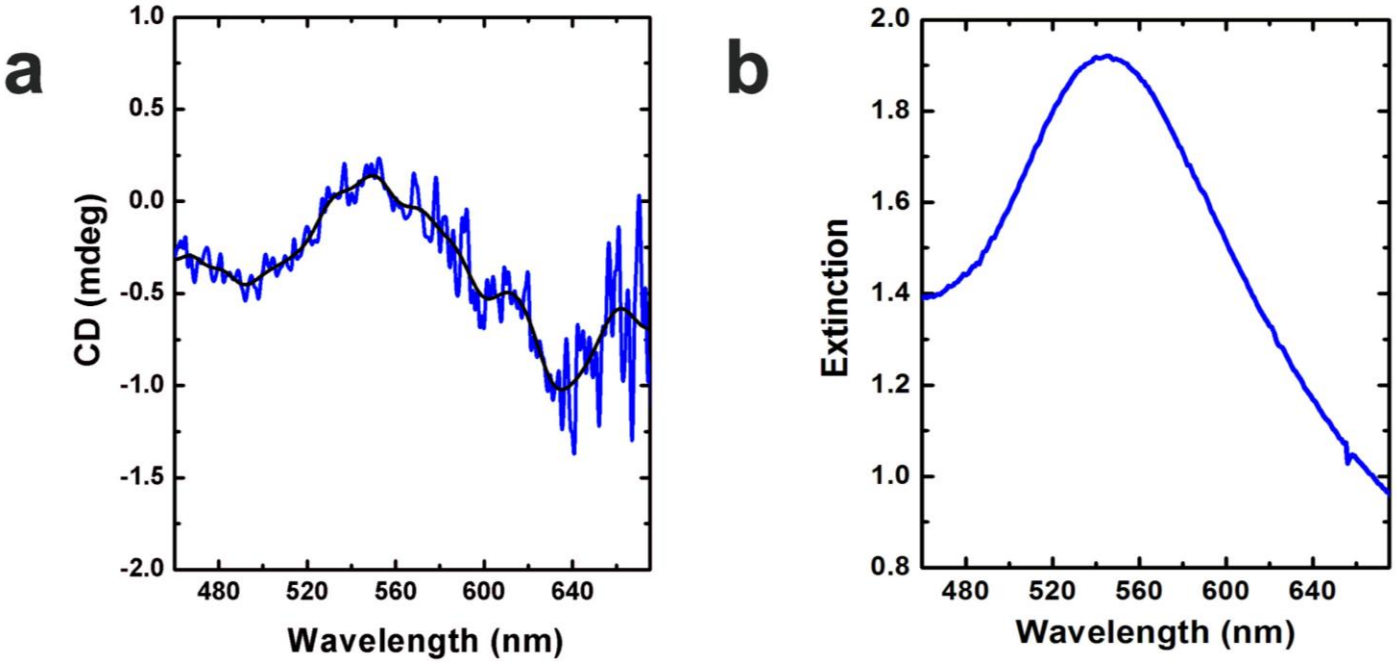

Figure S21. (a) CD spectrum of left-handed gold nanoparticle double helices incubated in 0.04 M citrate buffer and 0.06 M HEPES buffer for one day. The path length of the light is 1 mm. (b) UV-Vis spectrum of the left-handed gold nanoparticle double helices solution. It shows a surface plasmonic peak of gold assemblies at 545 nm which is consistent with the CD positive signal at 549 nm.

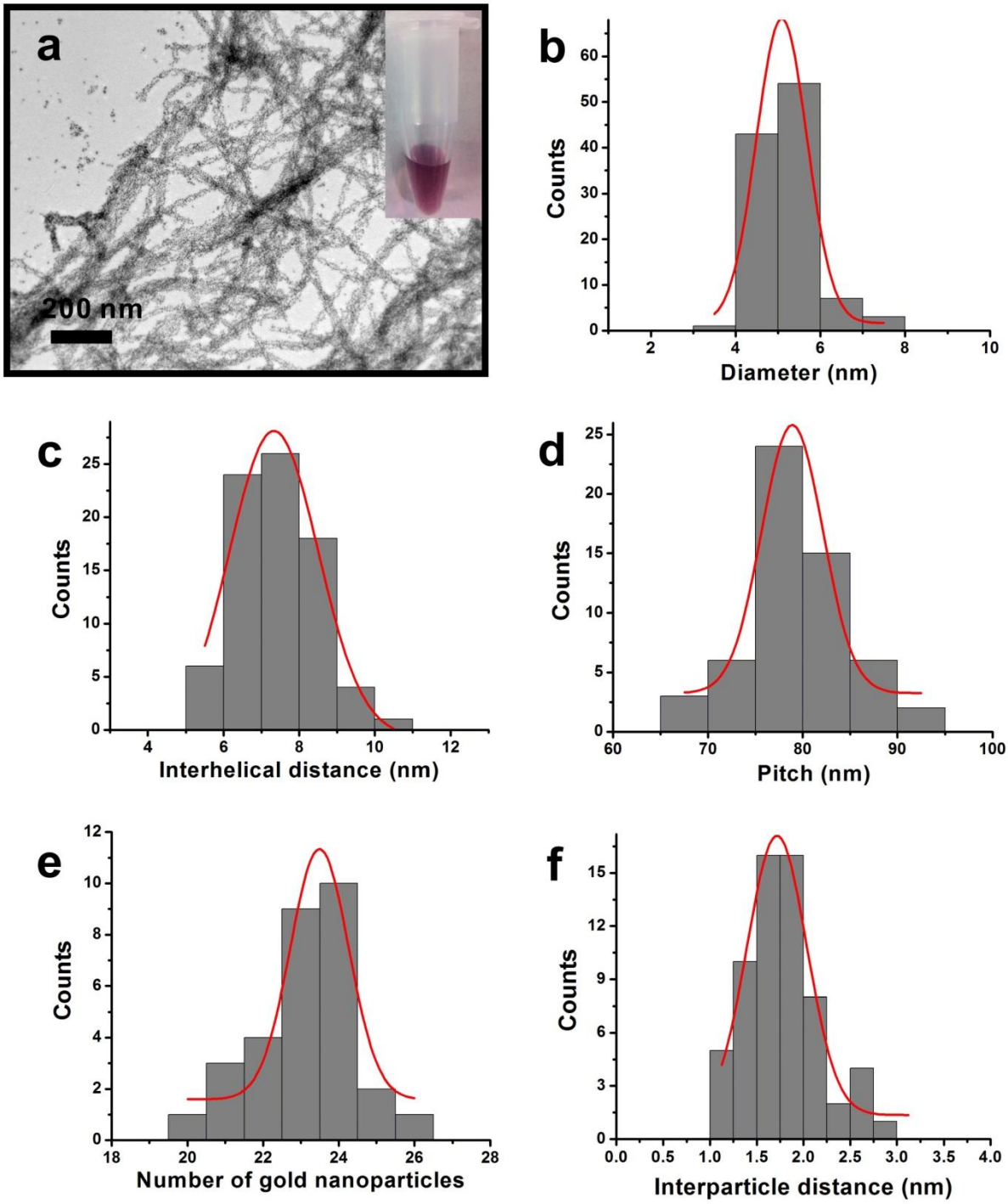

Figure S22. TEM image and statistics of left-handed gold nanoparticle double helices incubated in 0.04 M citrate buffer and 0.06 M HEPES buffer for one day. (a) TEM image of left-handed gold nanoparticle double helices. (b) Distribution of nanoparticle size (based on 108 counts; diameter = 5.09 ± 0.60 nm). (c) Distribution of the interhelical distance (based on 79 counts; distance = 7.33 ± 1.17 nm). (d) Distribution of pitch (based on 56 counts; pitch = 78.89 ± 3.23 nm). (e) Distribution of number of gold nanoparticles per pitch of double helix (based on 30 counts; number = 23 ± 2). (f) Distribution of the edge-to-edge distance between nanoparticles along the longitudinal dimension of the gold nanoparticle double helices (based on 62 counts; distance = 1.72 ± 0.32 nm).

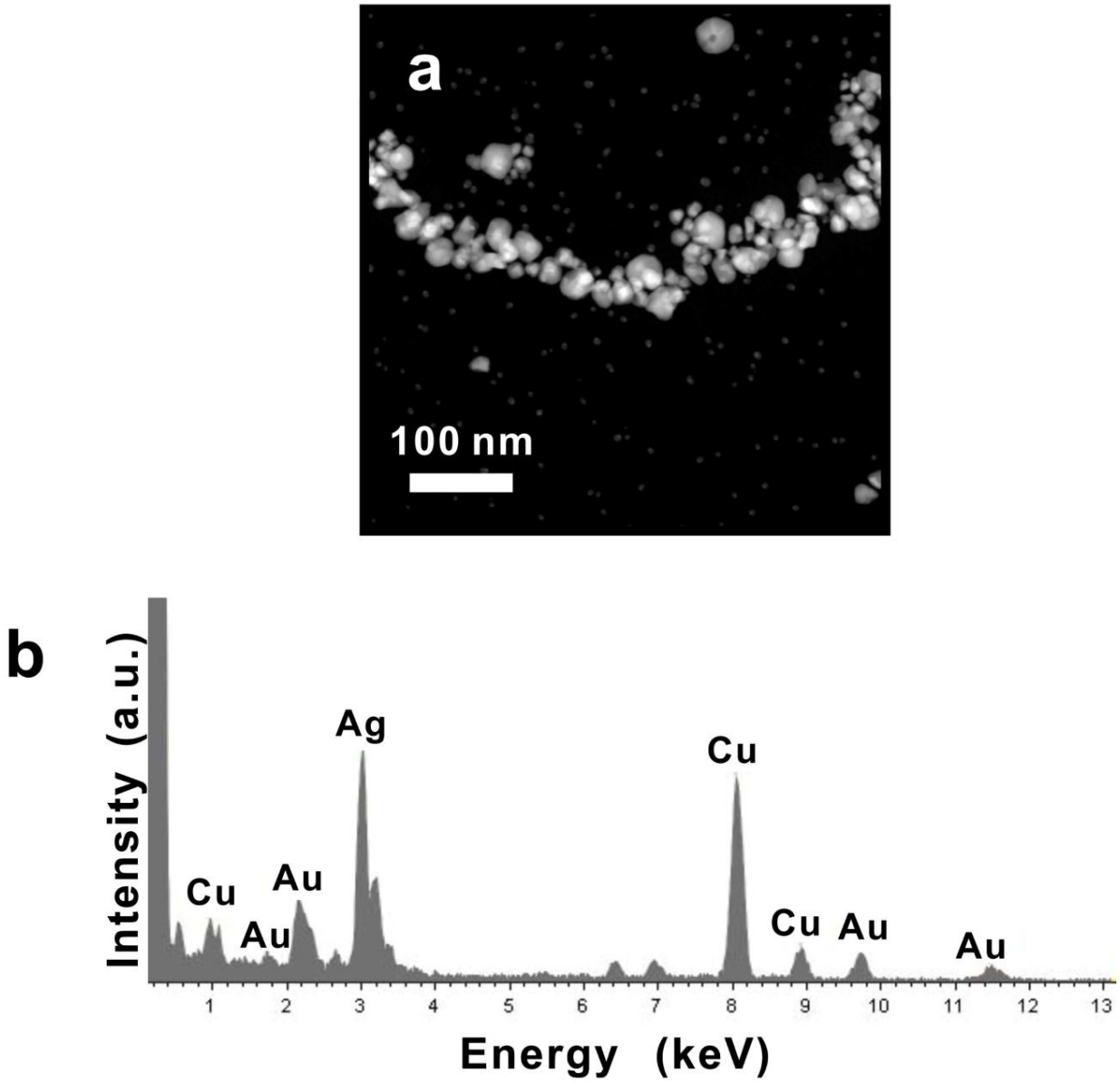

Figure S23. (a) STEM image of left-handed gold nanoparticle double helices enhanced by 108 μl Ag enhancer. It shows a white core (heavy metal:Au) surrounded by a gray shell (lighter metal: Ag). (b) EDS data of gold nanoparticle double helices (Cu is from the TEM grid).

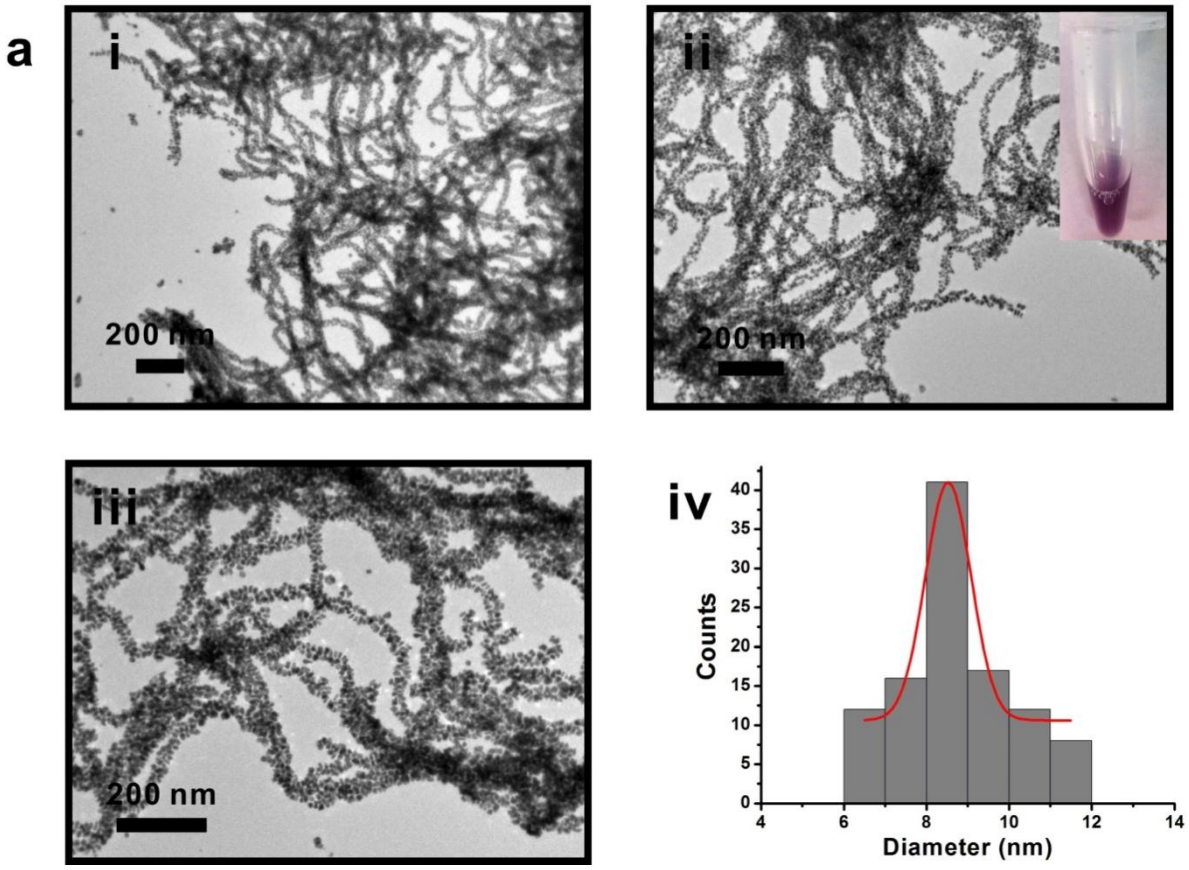

Figure S24a. (i-iii) TEM images of left-handed gold nanoparticle double helices enhanced with 9 μl Ag enhancer solution. The inset image of the vial shows the purple color of the gold nanoparticle double helices solution. (iv) Distribution of gold nanoparticle size on the double helices (based on 106 counts; diameter = 8.53 ± 0.55 nm).

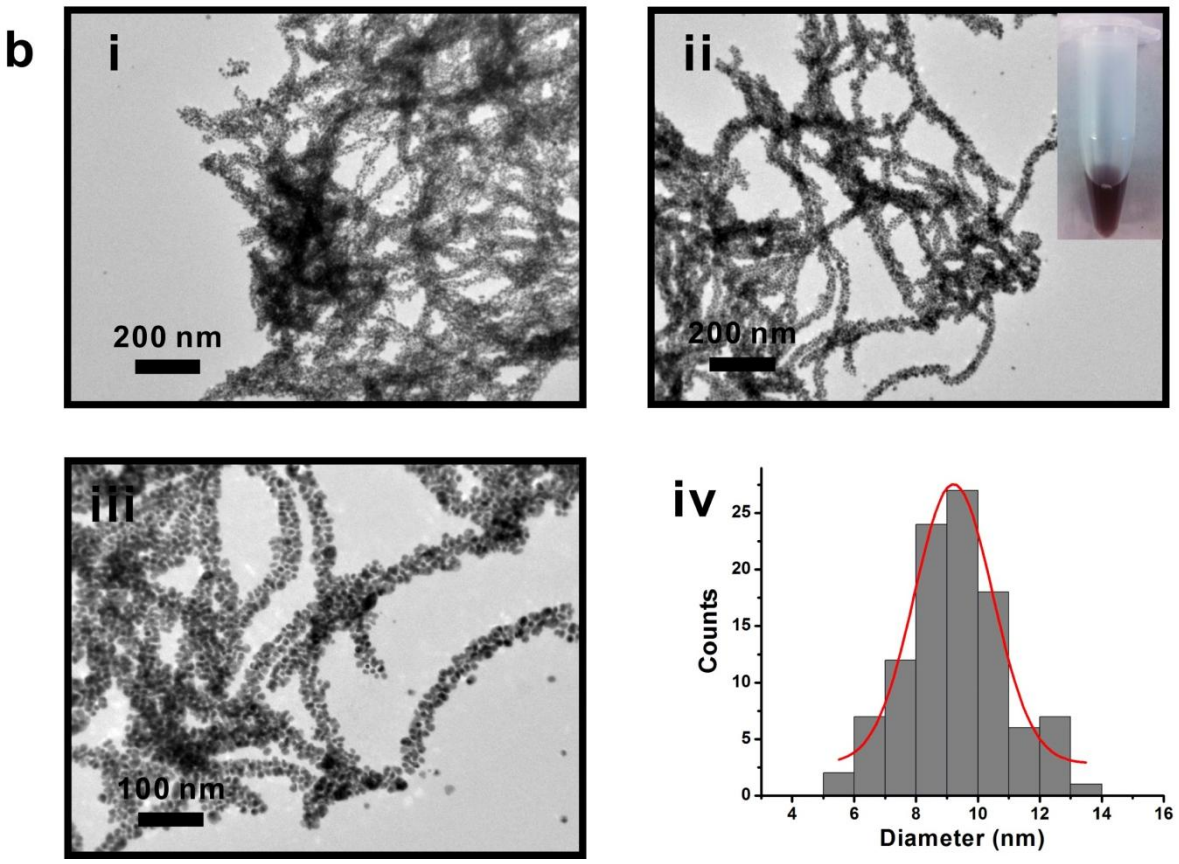

Figure S24b. (i-iii) TEM images of left-handed gold nanoparticle double helices enhanced with 27 μl Ag enhancer solution. The inset image of the vial shows the brown color of the gold nanoparticle double helices solution. (iv) Distribution of gold nanoparticle size on the double helices (based on 104 counts; diameter = 9.21 ± 1.27 nm).

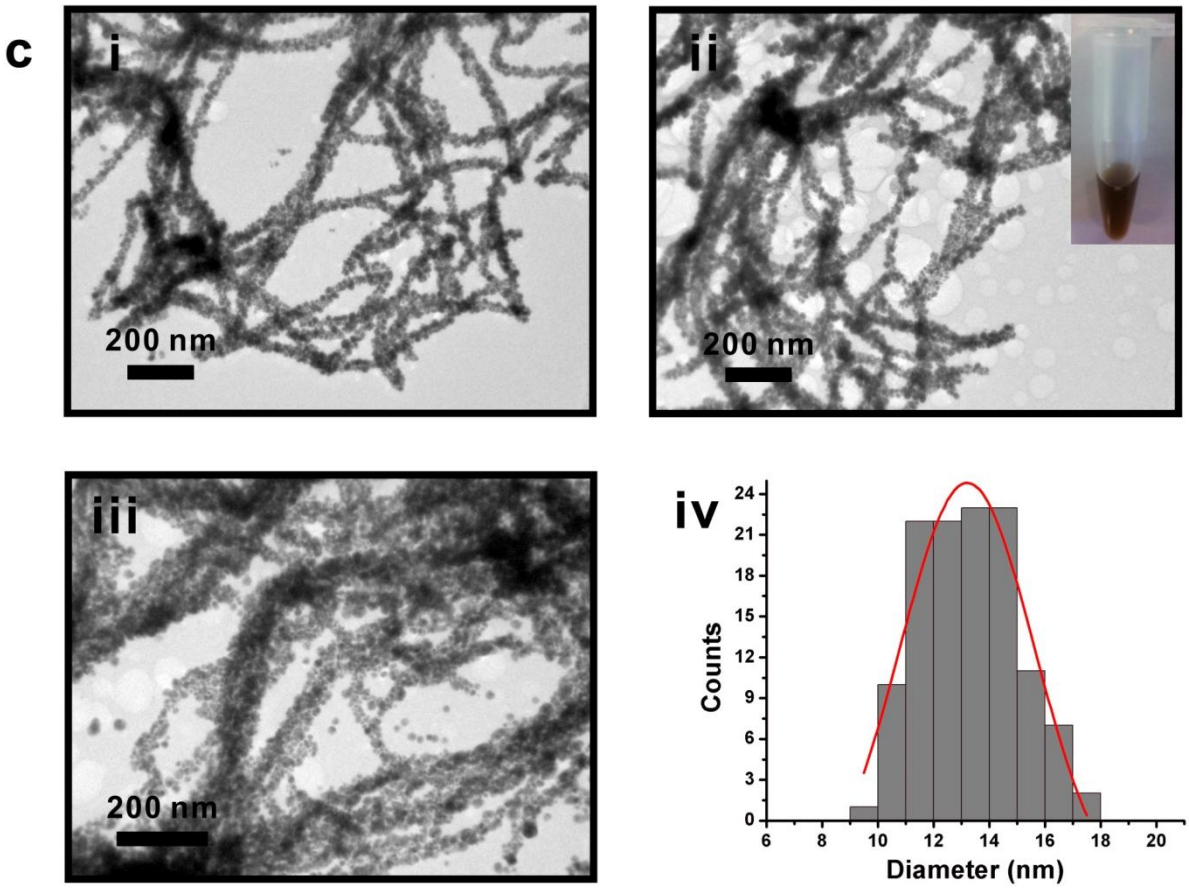

Figure S24c. (i-iii) TEM images of left-handed gold nanoparticle double helices enhanced with 54 µl Ag enhancer solution. The inset image of the vial shows the brown color of the gold nanoparticle double helices solution. (iv) Distribution of gold nanoparticle size on the double helices (based on 121 counts; diameter = 13.20 ± 2.41 nm).

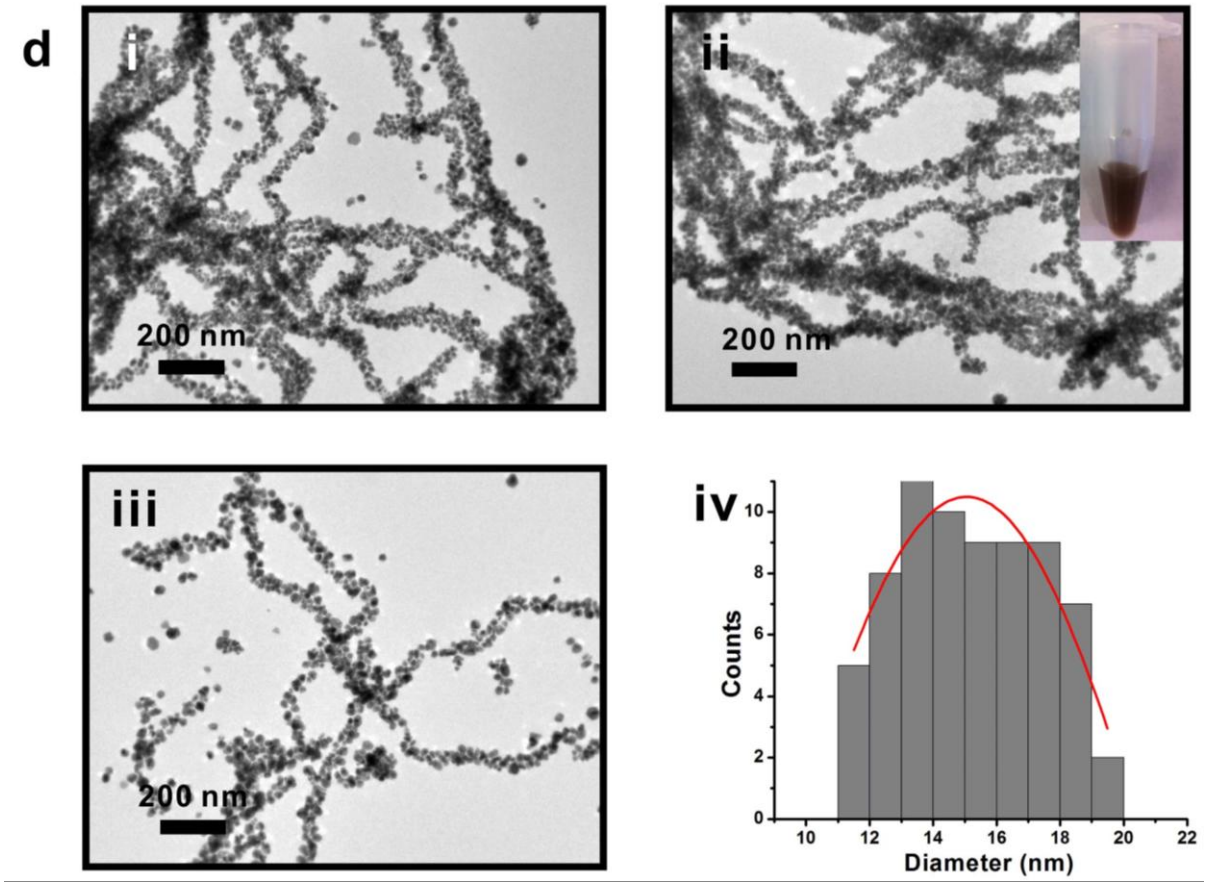

Figure S24d. (i-iii) TEM images of left-handed gold nanoparticle double helices enhanced with 108 μl Ag enhancer solution. The inset image of the vial shows the brown color of the gold nanoparticle double helices solution. (iv) Distribution of gold nanoparticle size on the double helices (based on 70 counts; diameter = 15.05 ± 6.90 nm).

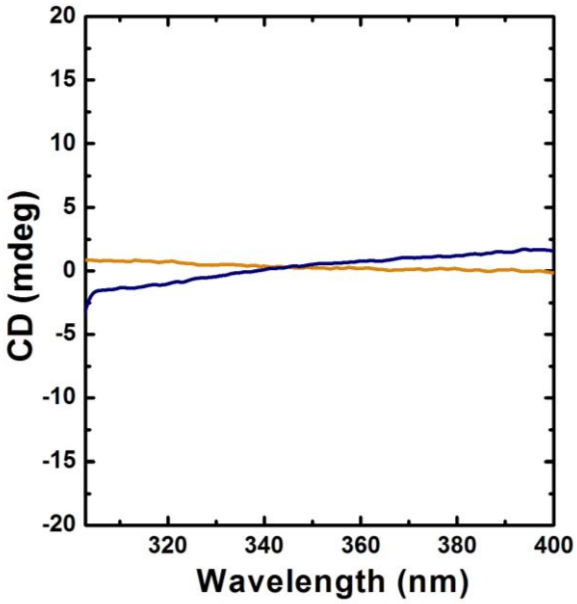

Figure S25. CD spectrum of left-handed gold nanoparticle double helices enhanced with 9 µl (orange) and 108 µl (blue) Ag enhancer solution within the UV region (300 nm – 400 nm). The path length of the light is 1 mm. (note: graphs are not corrected for dilution effects)

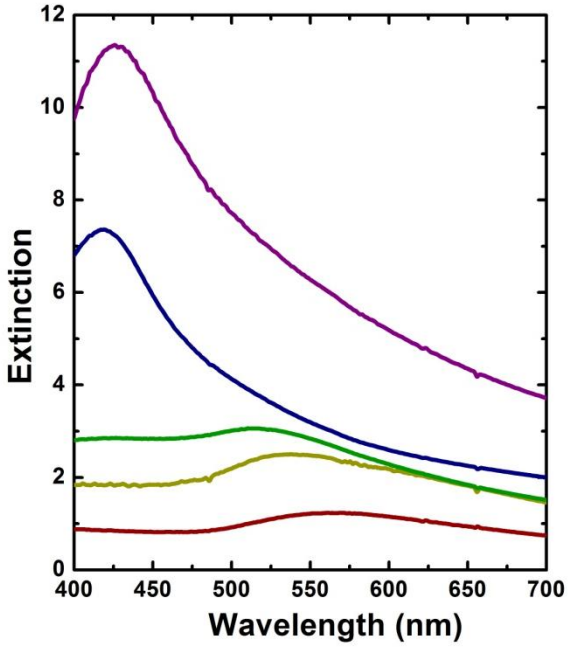

Figure S26. UV/Vis spectra of left-handed gold nanoparticle double helices solutions. No silver enhancement (red) and helices enhanced with 9 µl (yellow), 27 µl (green), 54 µl (blue) and 108 µl (purple) Ag enhancer solution within the visible region (400 nm – 700 nm). The path length of the light is 10 mm. (note: graphs are not corrected for dilution effects)

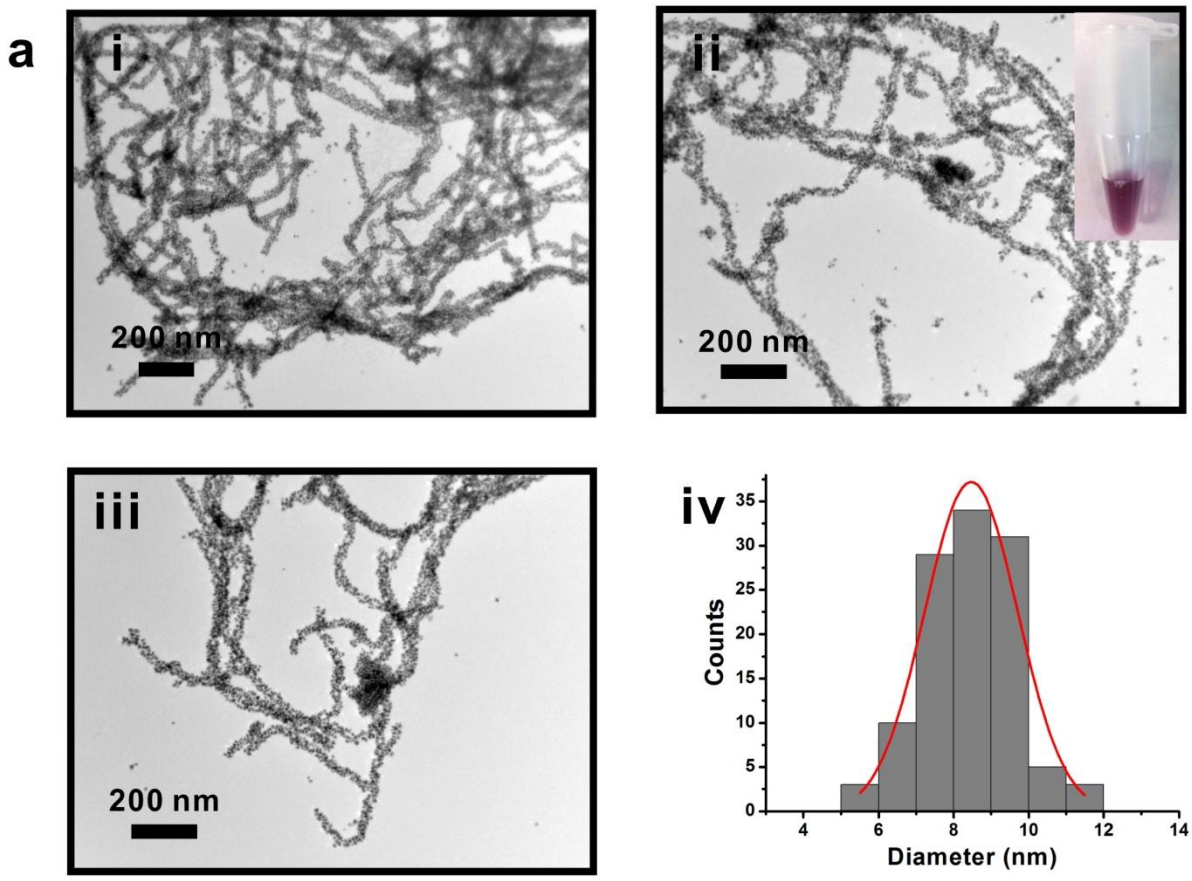

Figure S27a. (i-iii) TEM images of right-handed gold nanoparticle double helices enhanced with 9 μl Ag enhancer solution. The inset image of the vial shows the purple color of the gold nanoparticle double helices solution. (iv) Distribution of gold nanoparticle size on the double helices (based on 115 counts; diameter = 8.47 ± 1.24 nm).

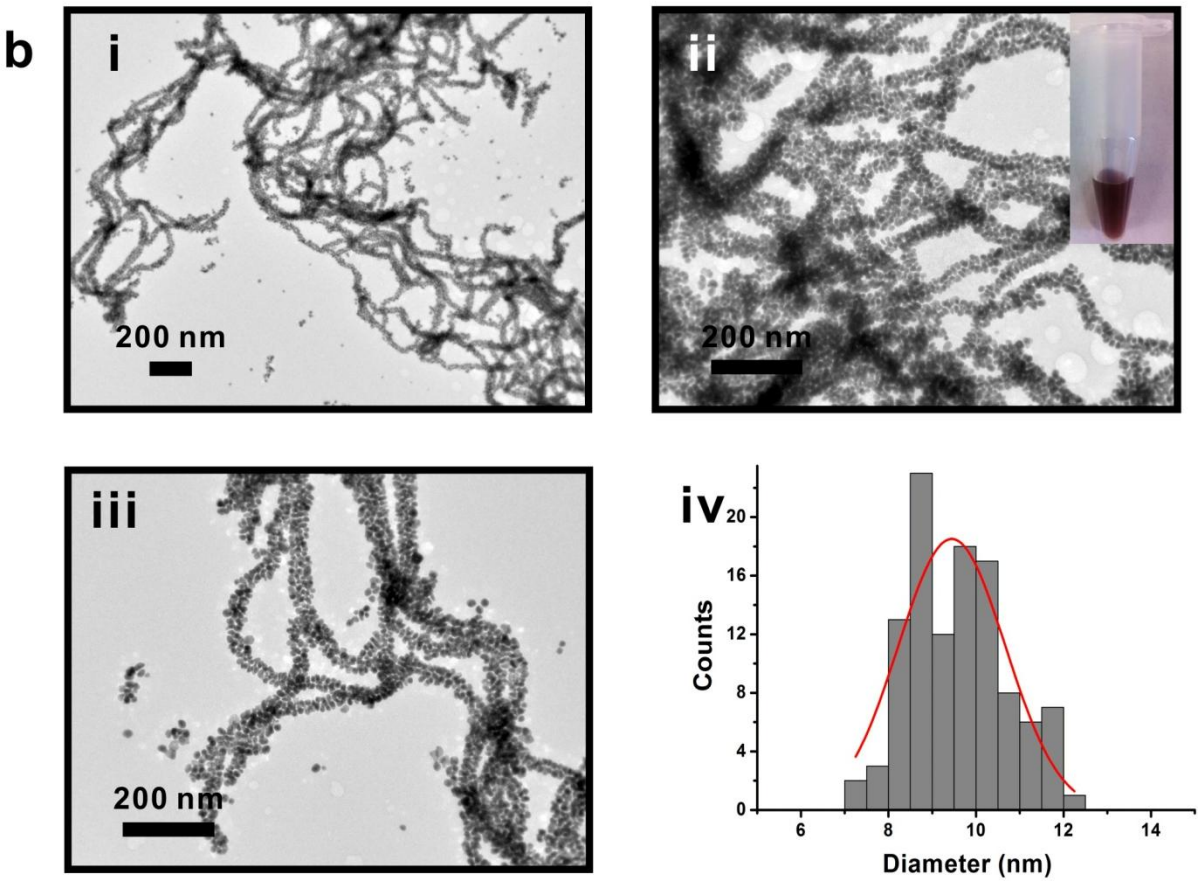

Figure S27b. (i-iii) TEM images of right-handed gold nanoparticle double helices enhanced with 27 μl Ag enhancer solution. The inset image of the vial shows the brown color of the gold nanoparticle double helices solution. (iv) Distribution of gold nanoparticle size on the double helices (based on 110 counts; diameter = 9.45 ± 1.23 nm).

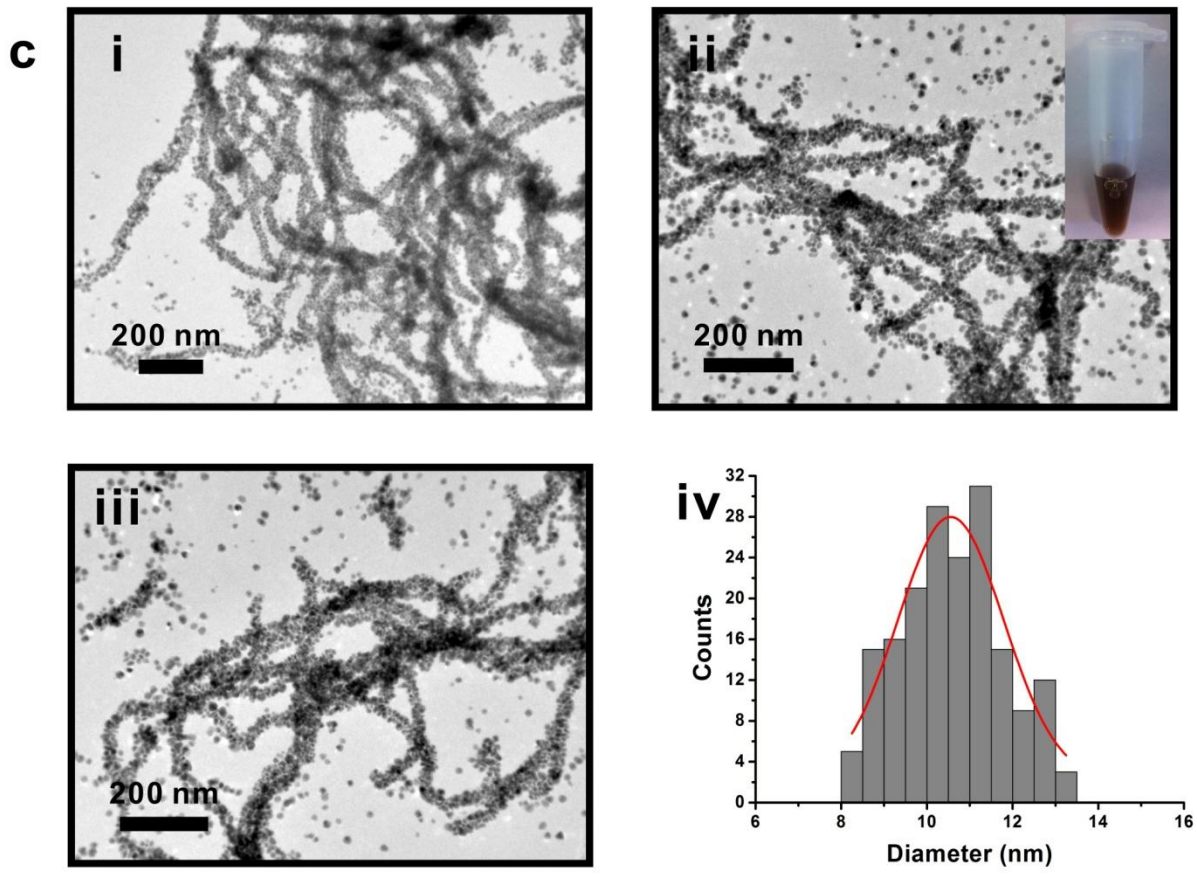

Figure S27c. (i-iii) TEM images of right-handed gold nanoparticle double helices enhanced with 54 µl Ag enhancer solution. The inset image of the vial shows the brown color of the gold nanoparticle double helices solution. (iv) Distribution of gold nanoparticle size on the double helices (based on 180 counts; diameter = 10.56 ± 1.24 nm).

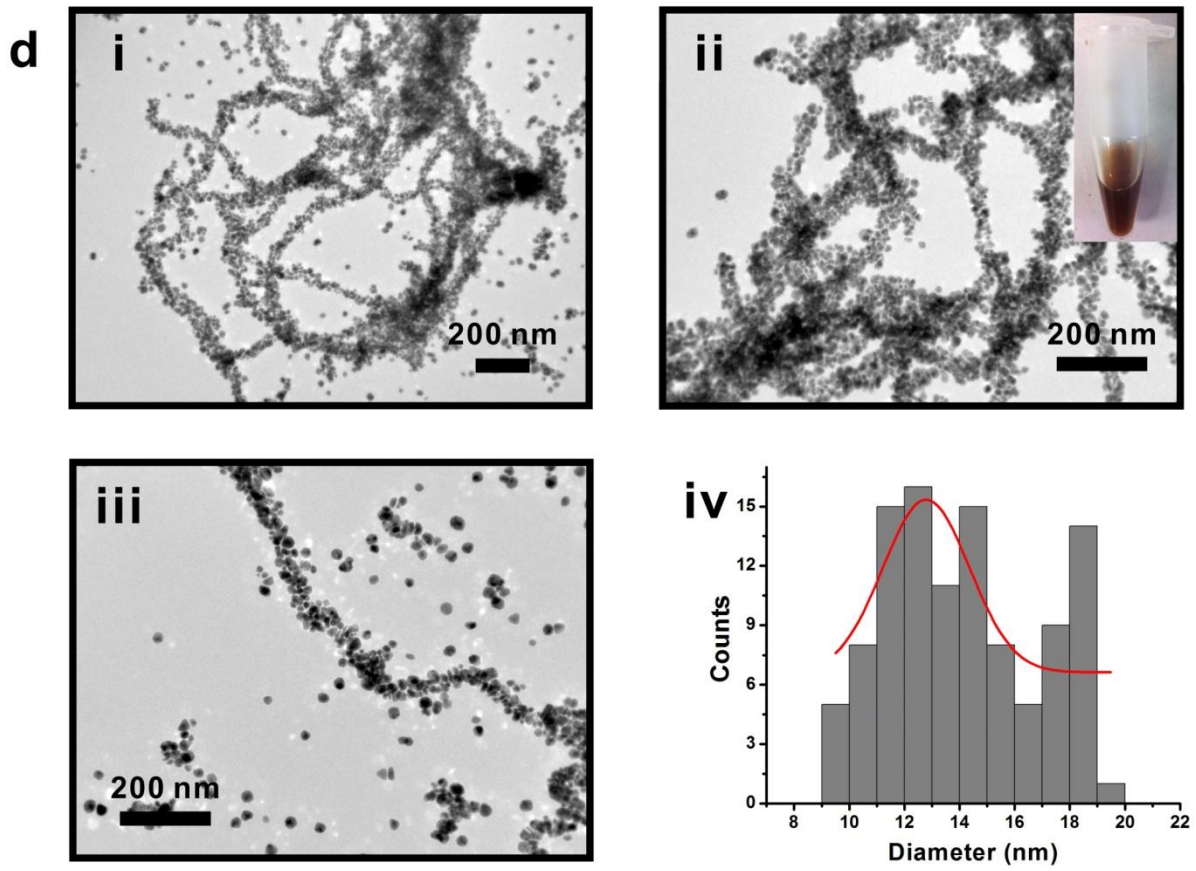

Figure S27d. (i-iii) TEM images of right-handed gold nanoparticle double helices enhanced with 108 μl Ag enhancer solution. The inset image of the vial shows the brown color of the gold nanoparticle double helices solution. (iv) Distribution of gold nanoparticle size on the double helices (based on 107 counts; diameter = 12.79 ± 1.57 nm).

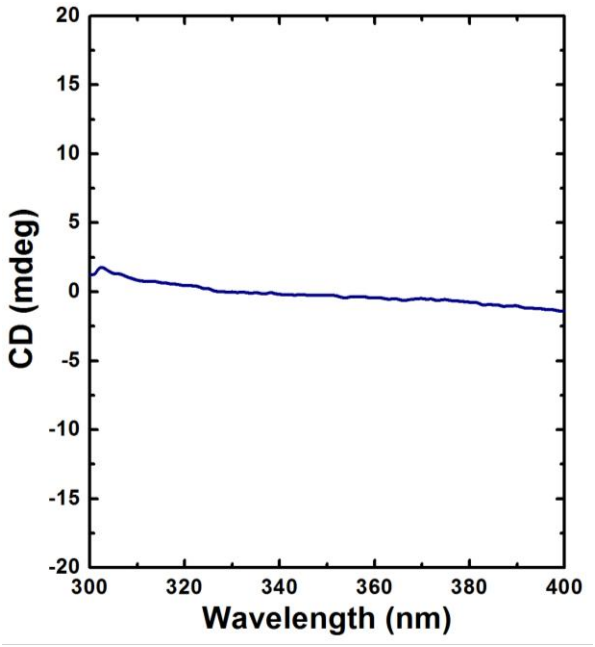

Figure S28. CD spectra of right-handed gold nanoparticle double helices enhanced with 108 µl Ag enhancer solution within UV region (300 nm – 400 nm). The path length of the light is 1 mm.

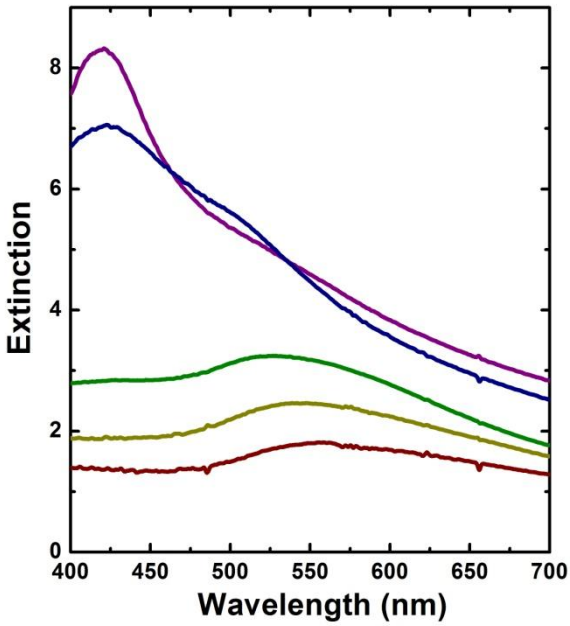

Figure S29. UV/Vis spectra of right-handed gold nanoparticle double helices solution. No silver enhancement (red) and helices enhanced with 9 µl (yellow), 27µl (green), 54 µl (blue) and 108 µl (purple) Ag enhancer solution within UV-Vis region (400 nm – 700 nm). The path length of the light is 10 mm. (note: graphs are not corrected for dilution effects).

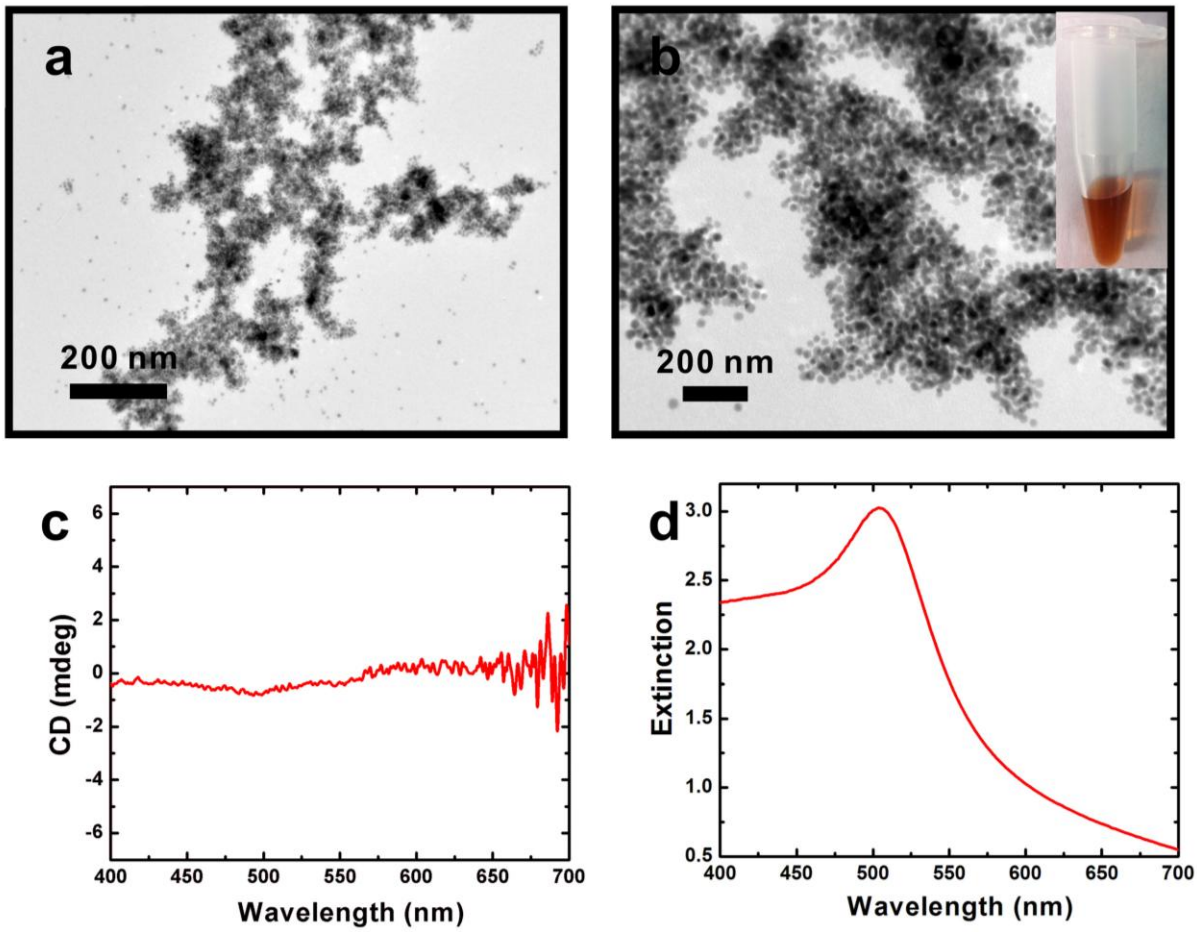

Figure S30. (a),(b) TEM images of PEP_{Au} capped free gold nanoparticles enhanced by 27 µl Ag enhancer solution. (Inset image shows the orange color of Ag enhanced free gold NP solution) (c) CD spectrum of Ag enhanced free gold NP solution. The path length of the light is 1 mm. (d) UV/Vis spectrum of Ag enhanced free gold NP solution. The surface plasmon peak is blue shifted to 503 nm compared with the typical peak (520 nm) of free gold NPs[17]. The path length of the light is 10 mm. (note: graphs are not corrected for dilution effects)

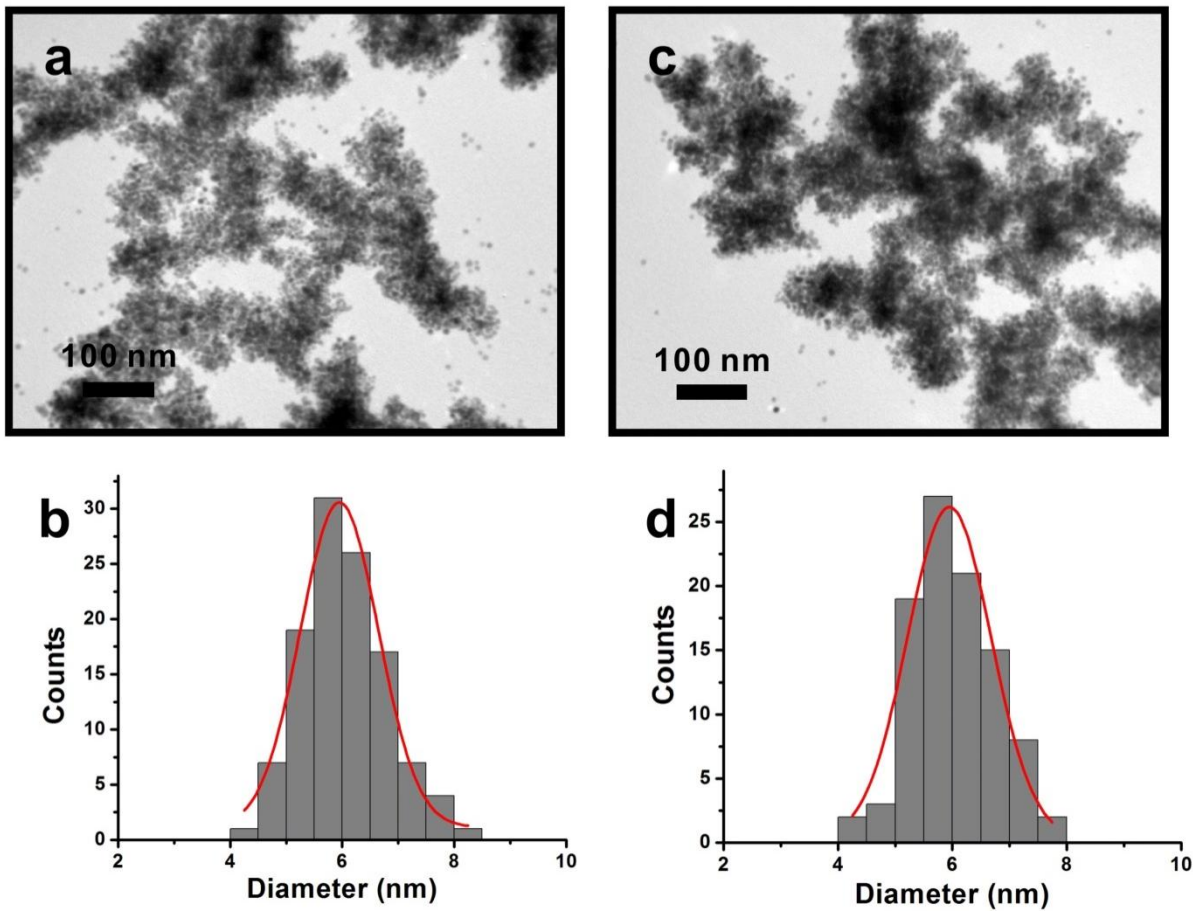

Figure S31. TEM images reveal that the size of silver coated gold nanoparticles is almost constant within one hour. (a) TEM image of PEP_{Au} capped free gold nanoparticles enhanced by 27 µl Ag enhancer solution incubating for one hour. (b) Distribution of size of Ag enhanced free gold NP solution after one hour incubation (based on 97 counts; diameter = 5.95 ± 0.73 nm). (c) TEM image of PEP_{Au} capped free gold nanoparticles enhanced by 27 µl Ag enhancer solution incubating for two hours. (d) Distribution of size of Ag enhanced free gold NP solution after two hours incubation (based on 113 counts; diameter = 5.95 ± 0.70 nm). We provide this comparison, because the CD data were collected on a sample that had been incubated with silver for 1 h. After the 1 h, the sample was taken to the instrument and CD was measured. We wanted to determine whether the particles would change significantly during transfer time and data collection time (after the 1 h incubation). This study indicates that the particles do not significantly change after the course of 1 h incubation with silver.

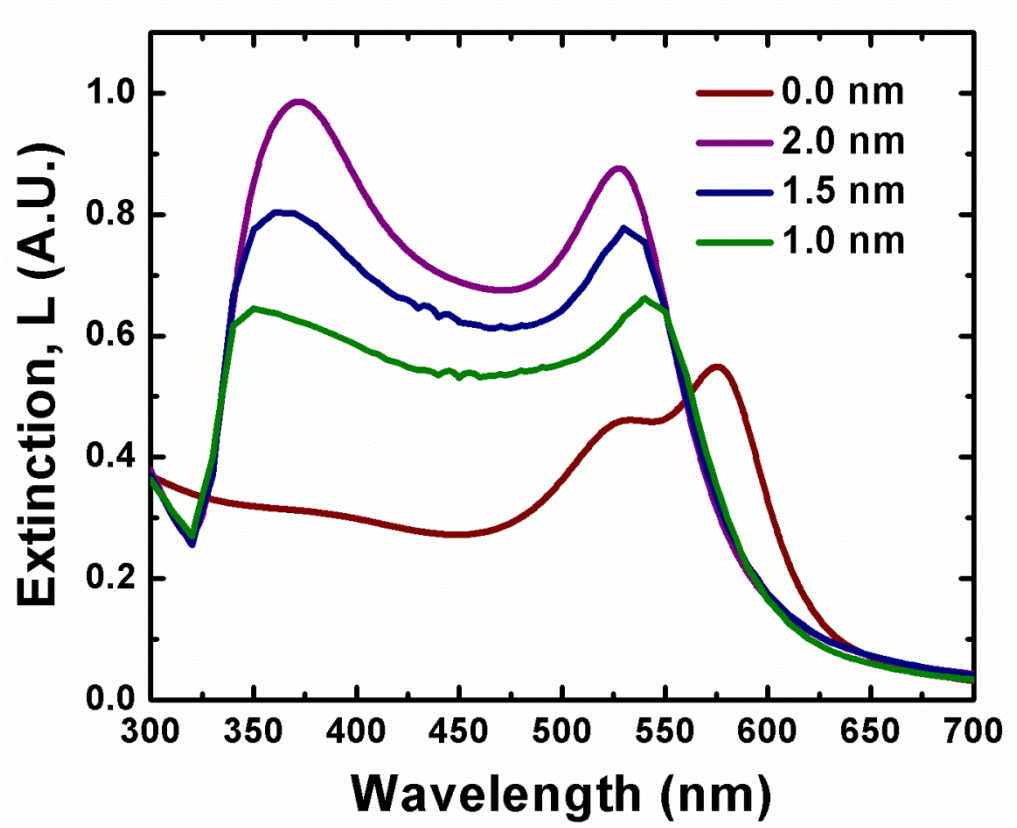

Figure S32. The simulated effect of silver shell thickness on the extinction of a double helix ensemble comprising 22 spheres. The silver shell thickness was sampled at 1.0 nm, 1.5 nm and 2.0 nm. The interhelical spacing is 7.0 nm, the gold sphere diameter is 8.0 nm and the interparticle spacing is 1.5 nm.

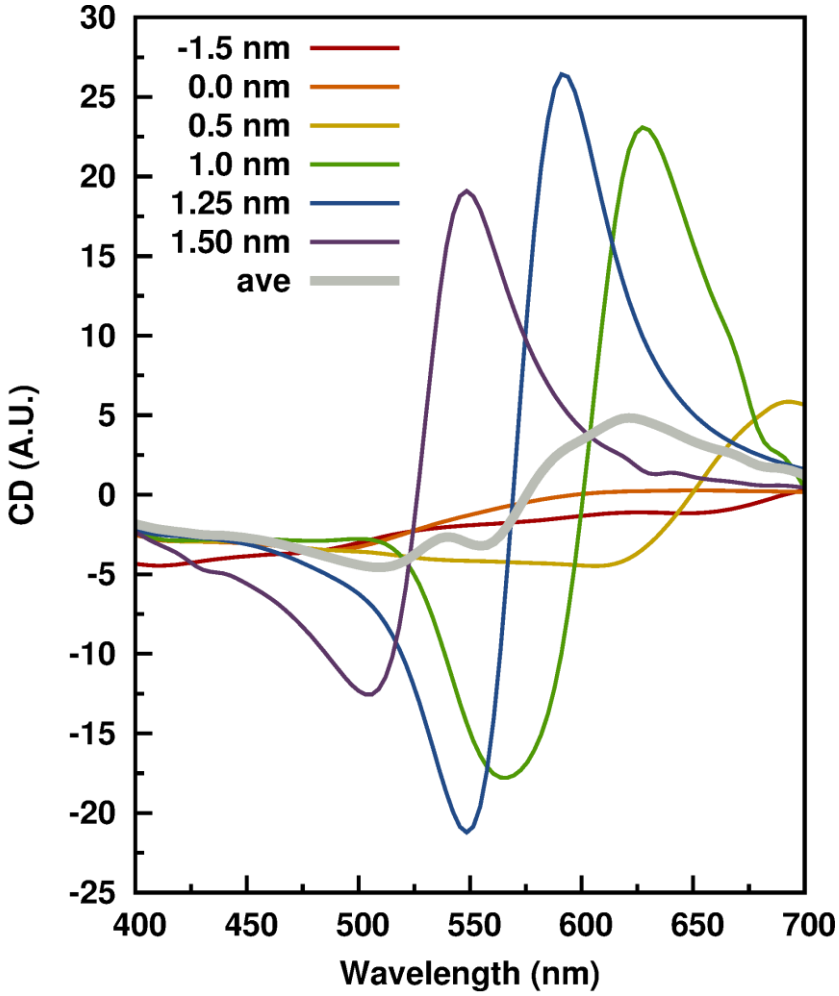

Figure S33. The simulated effect of interparticle gap of 4.0 nm radius gold spheres with 1.5nm silver shells on the CD response of a double helix ensemble comprising 22 spheres. The legend indicates the changing interparticle gap. When the gap is -1.5 nm, the shells overlap, and the gold cores are separated by 1.5 nm. The interhelical spacing is 7.0 nm. The figure shows that by averaging a distribution of interparticle spacings leads to an interference style effect that results in a flat CD response below 500 nm.

9. References

(1) Kremer, J. R.; Mastronarde, D. N.; McIntosh, J. R. *J. Struct. Biol.* **1996**, *116*, 71.
(2) Pettersen, E. F.; Goddard, T. D.; Huang, C. C.; Couch, G. S.; Greenblatt, D. M.; Meng, E. C.; Ferrin, T. E. *J. Comput. Chem.* **2004**, *25*, 1605.
(3) Draine, B. T.; Flatau, P. J. *J Opt Soc Am A* **1994**, *11*, 1491.
(4) Draine, B. T.; Flatau, P. J. *arXiv:1202.3424 [physics.comp-ph]* **2012**.
(5) Yang, W. H.; Schatz, G. C.; Van Duyne, R. P. *Discrete dipole approximation for calculating extinction and Raman intensities for small particles with arbitrary shapes*; AIP, 1995; Vol. 103.
(6) Gutkowicz-Krusin, D.; Draine, B. T. *arXiv:astro-ph* **2004**, *0403082v1*.
(7) Draine, B. T.; Goodman, J. *Astrophys J* **1993**, *405*, 685.
(8) Johnson, P. B.; Christy, R. W. *Phys. Rev. B* **1972**, *6*, 4370.
(9) Kreibig, U.; Fragstein, C. v. *Zeitschrift fur Physik A Hadrons and Nuclei* **1969**, *224*, 307.
(10) Brioude, A.; Jiang, X. C.; Pileni, M. P. *J. Phys. Chem. B* **2005**, *109*, 13138.
(11) Goodman, J. J.; Draine, B. T.; Flatau, P. J. *Opt. Lett.* **1991**, *16*, 1198.
(12) Du, Q.; Faber, V.; Gunzburger, M. *SIAM Rev.* **1999**, *41*, 637.
(13) Hardin, D. P.; Saff, E. B. *Notices Amer. Math. Soc.* **2004**, *51*, 1186.
(14) Renka, R. J. *ACM T Math. Software* **1997**, *23*, 416.
(15) Saff, E. B.; Kuijlaars, A. B. J. *Math. Intell.* **1997**, *19*, 5.
(16) Chen, C.-L.; Zhang, P.; Rosi, N. L. *J. Am. Chem. Soc.* **2008**, *130*, 13555.
(17) Link, S.; El-Sayed, M. A. *J. Phys. Chem. B* **1999**, *103*, 8410.